Journal of Applied Mathematics and Physics, 2023, 11, 3287-3314
https://www.scirp.org/journal/jamp
ISSN Online: 2327-4379
ISSN Print: 2327-4352

Magneto-Hydrodynamic Flow of an Incompressible Fluid in a Collapsible Elastic Tube with Mass and Heat Transfer

Victor Kaigalula[1*], Jeconia Okelo[2], Samuel Mutua[3], Onesmus Muvengei[4]

[1]Department of Mathematics, Pan African University Institute of Basic science, Technology and Innovation, Nairobi, Kenya
[2]Department of Pure and Applied Mathematics, Jomo Kenyatta University of Agriculture and Technology, Nairobi, Kenya
[3]Mathematics, Statistics and Physical Sciences Department, Taita Taveta University, Nairobi, Kenya
[4]Department of Mechanical, Manufacturing and Materials Engineering, Jomo Kenyatta University of Agriculture and Technology, Nairobi, Kenya
Email: *kaigalula119@gmail.com

How to cite this paper: Kaigalula, V., Okelo, J., Mutua, S. and Muvengei, O. (2023) Magneto-Hydrodynamic Flow of an Incompressible Fluid in a Collapsible Elastic Tube with Mass and Heat Transfer. *Journal of Applied Mathematics and Physics*, **11**, 3287-3314.
https://doi.org/10.4236/jamp.2023.1111211

Received: October 4, 2023
Accepted: November 3, 2023
Published: November 6, 2023

Abstract

The aim of this study is to examine unsteady incompressible Magnetohydrodynamic fluid flow together with soret and dufour effects on mass and heat transfer through a collapsible elastic tube. The governing equations are continuity equation, momentum equation, energy equation and concentration equation. The velocity, temperature and concentration profiles together with heat and mass transfer rate were determined. The system of nonlinear partial differential equations governing the flow solved numerically by applying collocation method and implemented in MATLAB. The numerical solution of the profiles displayed both by graphically and numerically for different values of the physical parameters entering into the problem. The effects of varying various parameters such as Reynolds number, Hartmann number, Soret number, Dufour number and Prandtl number on velocity, temperature and concentration profiles also the rate of heat and mass transfer are discussed. The study is significant because heat and mass transfer mechanisms with the soret and dufour effects considerations play an important role due to its wide range of application including but not limited to medical fields, biological sciences and other physical sciences where collapsible tubes are applied.

Keywords

Collapsible Tube, Magnetohydrodynamics, Soret-Dufour, Joule Heaing, Collocation Method

1. Introduction

Collapsible tubes are tube with circular cross-section which is able to accommodate elastically deformation when exposed to internal-external pressure difference or flow variance refered to as transmural pressure. The entire tubes in human body are flexible and also made of collapsible walls. The study of the magnetic characteristics and behavior of electrically conducting fluids is known as hydromagnetics alternatively magneto-hydrodynamics (MHD). MHD fluid flow through collapsible elastic tube with mass and heat transfer is of utmost importance due to its application in sciences and engineering. The study involving Magneto-hydrodynamic flow through a collapsible tube with mass and heat transfer can be used to solve practical problems in field like medicine, engineering and so on. However, the effect of heat and mass transfer through a collapsible elastic tube has received little attention. This tubes are very important in our daily life due to it involves in different areas such as in biological studies, veins, arteries, urethra and airways tubes are examples of collapsible elastic tube. The experimental and theoretical research on unsteady incompressible MHD flows is important to scientific and engineering fields in particular biological flows such as blood flow in arteries or veins, flow of urine in urethra and air flow in the bronchial airways. Also can be used to study and prediction of many diseases such as the lung disease (asthma and emphysema), or cardiovascular diseases (heart stroke). Also important in engineering processes such as in MHD power generators for electricity production, accelerators, MHD pumps, MHD flow meters, electrostatic filters, the design of cooling systems with liquid metals, and in geothermal power stations. In the human body, collapsible tubes such as blood vessels, bronchioles, and ureters play important roles in the transport of fluids. Blood is essential in sustaining life as it transport oxygen and nutrients to all parts of the body, relays chemical signals and moves metabolic wastes to the kidney for elimination. Similarly in the industries collapse may be experienced during cementing operations, trapped fluid expansion or well evaculation. Quantitative models of fluid flows are important, to date numerous mathematical models have been developed describing MHD fluid flow in different areas but few have done in collapsible tube. Research done by [1] investigate mathematical model describing fluid dynamics in a collapsible tube, he constructed analytical solution for problem using pertubation technique and Hermite-Pade approximations. [2] analyzes the unsteady behavior and linear stability of the flow in a Collapsible tube by using a fluid beam model. [3] established Soret and Dufour effects on free convection heat and mass transfer from horizontal flat plate in a Darcy porous medium. [4] examined an incompressible viscous fluid flow and heat transfer in a collapsible tube. [5] analyze Soret and Dufour effect on natural convection heat and mass transfer from a vertical cone in a porous medium. [6] develop three-dimensional computer model to simulate fluid flow through a collapsible tube. [7] investigated an accurate modeling of unsteady flows in collapsible tubes. One-dimensional Runge-Kutta discontinuous Galerkin method

coupled with lumped parameter models for the boundary conditions was used. [8] studied soret and dufour effects on heat and mass transfer due to a stretching cylinder saturated porous medium which chemically reactive species. [9] studied fluid flow in collapsible tubes with discontinuous mechanical properties. [10] combined effects of Soret (thermal-diffusion) and Dufour (diffusion-thermo) on a mixed convection over a stretching sheet embedded in a saturated porous medium in the presence of thermal radiation and chemical reaction studied. It was found that temperature profiles increase with increase in Dufour number. [11] investigate Soret and dufour effects on MHD convective heat and mass transfer of a power-law fluid over an inclined plate with variable thermal conductivity in a porus medium. Nonlinear ordinary differential equations are solved numerically based on shooting method with Runge-Kutta Fehlberg integration scheme.

[12] investigated multiple states for flow through a Collapsible tube with discontinuities. It was established that the complexity of the fluid-structure gives Collapsible tubes their specific dynamic features. The numerical solution was obtained by using finite volume method of the path conservative type.

[13] studied the effects of flow parameters (tube stiffiness and longitudinal tension) on the flow variables of a Newtonian, steady incompressible fluid flowing through cylindrical collapsible tube. The result shows that the flow parameter considered are directly proportional to both the cross sectional area and internal pressure and inversely proportional to the flow velocity. [14] in this study, an incompressible viscous fluid flow and heat transfer in a collapsible tube with heat source or sink is examined. [15] described unsteady MHD fluid flow in a collapsible tube. The fluid was considered to be Newtonian. The non linear partial differential equations which were solved numerically using finite difference method (FDM). [16] investigated steady low Reynolds number flow of a generalized Newtonian fluid through a slender elastic tube. [17] investigate a study of two dimensional unsteady MHD free convection flow over a vertical plate in the presence of radiation. They examine radiactive effects on the MHD free convection flow of an electrically conducting incompressible viscous fluid over a vertical plate. Dimensionless momentum and energy equations were solved numerically by using explicit finite difference method. It was established that velocity profiles decreases with an increasing Grashof number. Also there was decline of velocity profiles because of increasing values of Eckert number as a result heat transfer of the flow reduced the driving force to the kinetic energy.

[18] examine heat transfer of helical coil in heat exchangers (HCHE). It demonstrated that the helical heat exchanger provide more excellent heat transfer performance and effectiveness than straight tubes. It was obtained that heat transfer coefficient increased with an increase in curvature ratio of HCHE fot the same flow rates. [19] investigated analytical modelling of an unsteady fluid flow through an elastic tube. The fluid was considered to be Newtonian and Incompressible, they took into consideration large Reynolds number and a small aspect ratio, the tube was assumed to be having a small shell, which they considered to

be the source of asymmetric vibration. [20] investigated unsteady flow of Newtonian fluid in collapsible tube. They formulated a mathematical model of a Newtonian fluid in a collapsible tube to simulate physiological flows such as flow of blood and urine within human body system. [21] investigated fluid flow coupled with heat transfer through a vertical cylindrical collapsible tube in the presence of magnetic field and an obstacle. [22] investigated numerical solution of blood flow and mass transport in an elastic tube with multiple stenosis. [23] investigate effects of thermophoresis, Soret-Dufour on heat and mass transfer flow of magnetohydrodynamics non-Newtonian nanofluid over an inclined plate. [24] investigated the unsteady flow of collapsible tube under transverse magneto hydrodynamic fluid. Their aim was to determine the velocity and temperature profiles, and the effects of some non-dimensional numbers of the taken nanofluid. [25] analyze numerical investigation on the heat and mass transfer in microchannel with discrete heat sources considering the Soret and Dufour effects. [26] investigate Heat transfer of MHD flow over a Wedge with Surface of Mutable temperature. [27] investigate Numerical simulation of MHD two-dimensional flow incorporated with joule heating and nonlinear thermal radiation. This type of problem is critical for fluid flows in capillary tubes such as blood flow in arteries or veins. This can result inefficient transport of nutrients, waste products, and other substances throughout the body.

Numerous studies have been conducted on hydromagnetic fluid flows with various factors taken into consideration as illustrated above, however, not much attention has been given to the soret and dufour effects on unsteady hydrodynamic fluid flow through a collapsible elastic tubes. Therefore this paper focused to investigate the combined effects of Soret-Dufour effects together with Joule heating on unsteady incompressible MHD flow with mass and heat transfer through a collapsible tube.

2. Mathematical Formulation

This study consider two dimension MHD flow with mass and heat transfer that takes place along r and z-directions, then u_r and u_z are velocity components in r and z direction respectively with B_0 as magnetic field strength and g is acceleration due to gravity. The collapsible elastic tube is cylindrical whereby the z axis lies along the center of the collapsible elastic tube. **Figure 1** below shows a sketch diagram of the research problem.

The fluid flow is laminar and newtonian. The induced magnetic field, external electric field and Hall current are negligible. The difference in internal-external pressure is constant throughout the tube. The governing equations are continuity, momentum, energy and Concentration which are given respectively as:

Continuity equation:

$$\frac{\partial u_z}{\partial z} = 0 \tag{2.1}$$

Momentum equation:

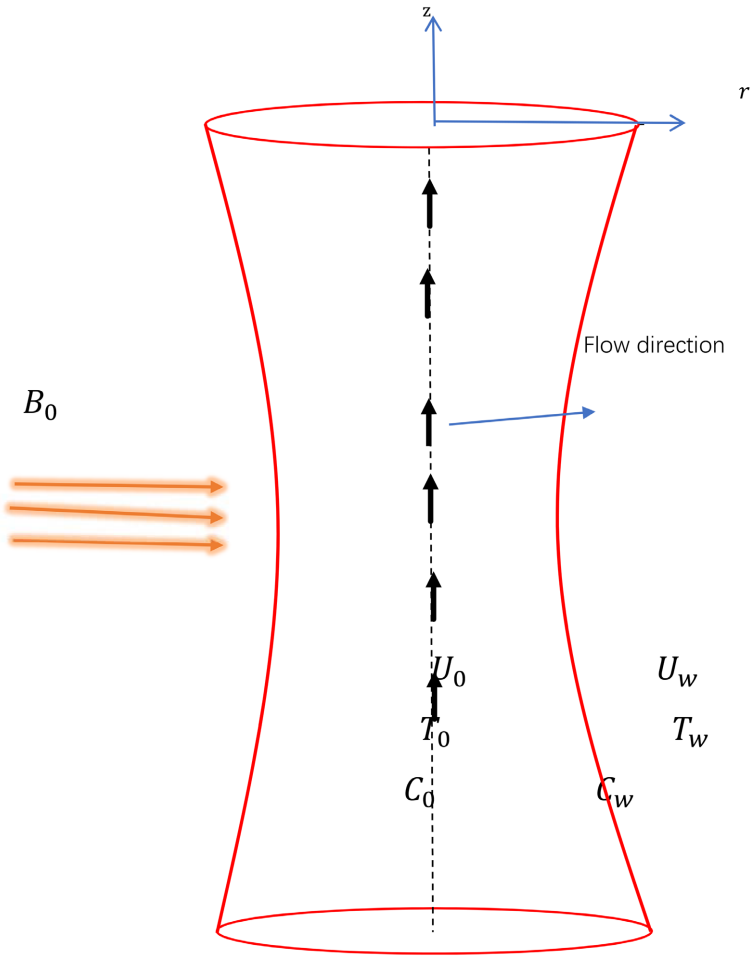

Figure 1. Physical Model of the problem.

$$\frac{\partial u_z}{\partial t}=\frac{\mu}{\rho}\left[\frac{\partial^2 u_z}{\partial r^2}+\frac{1}{r}\frac{\partial u_z}{\partial r}\right]-\frac{\sigma B_0^2 u_z}{\rho}+\beta' g\left(T-T_w\right)+\beta^c g\left(C-C_w\right) \tag{2.2}$$

Energy equation:

$$\left(\frac{\partial T}{\partial t}+u_z\frac{\partial T}{\partial z}\right)=\frac{\kappa}{\rho C_p}\left(\frac{\partial^2 T}{\partial r^2}+\frac{1}{r}\frac{\partial T}{\partial r}+\frac{\partial^2 T}{\partial z^2}\right)+\frac{\mu}{\rho C_p}\left(\frac{\partial u_z}{\partial r}\right)^2 +\frac{\sigma u_z^2 B_0^2}{\rho C_p}+\frac{D_m K_t}{C_p C_s}\left(\frac{\partial^2 C}{\partial r^2}+\frac{1}{r}\frac{\partial C}{\partial r}+\frac{\partial^2 C}{\partial z^2}\right) \tag{2.3}$$

Concentration equation:

$$\frac{\partial C}{\partial t}=-u_z\frac{\partial C}{\partial z}+D_m\left[\frac{\partial^2 C}{\partial r^2}+\frac{1}{r}\frac{\partial C}{\partial r}+\frac{\partial^2 C}{\partial z^2}\right]-k_r\left(C-C_w\right) +\frac{D_m K_t}{T_m}\left(\frac{\partial^2 T}{\partial r^2}+\frac{1}{r}\frac{\partial T}{\partial r}+\frac{\partial^2 T}{\partial z^2}\right) \tag{2.4}$$

Boundary conditions considered are as follows.

At the centre line of the tube,

$$u_z=U_0,\quad T=T_0,\quad C=C_0,\quad r=0 \tag{2.5}$$

At the wall,

$$u_z = 0, \quad T = T_W, \quad C = C_W, \quad r = a(t) \tag{2.6}$$

The following non-dimensional transformation are used in the equation of continuity, equation of momentum, energy and concentration as used by ([21] [28] [29] and [30])

$$u_z = -\frac{Q}{z}\cdot\frac{1}{\delta^{m+1}}f(\eta), \quad \frac{\omega(\eta)}{\delta^{m+1}} = \frac{T-T_w}{T_0-T_w}, \quad \frac{\omega(\eta)_c}{\delta^{m+1}} = \frac{C-C_w}{C_0-C_w}, \quad \eta = \frac{r}{a_0} \tag{2.7}$$

where $f(\eta)$ is the dimensionless velocity, $\omega(\eta)$ is the dimensionless temperature and $\omega(\eta)_c$ is the dimensionless concentration, T_0 is the temperature at the center of the tube, T_w is the temperature at the wall, C_0 is the Concentration at the center of the tube, C_w is the concentration at the wall, δ is the time dependent length scale and η, m are arbitrary constant.

The following obtained,

$$\begin{aligned} &f''(\eta)+\frac{1}{\eta}f'(\eta)+\frac{a_0^{m+1}(m+1)}{\delta^{m+1}}\lambda f(\eta)-\frac{\sigma B_0^2 a_0^2}{\mu}f(\eta)\\ &-\frac{a_0^2 z\delta^{m+1}}{vQ}\left[\beta^t g(T-T_w)+\beta^c g(C-C_w)\right]=0 \end{aligned} \tag{2.8}$$

$$\begin{aligned} &-\frac{(m+1)a_0^{m-1}}{\delta^{m+1}}\lambda\omega(\eta)=\frac{\kappa}{\mu_0 C_p}\left(\frac{1}{a_0^2}\omega''(\eta)+\frac{1}{a_0^2\eta}\omega'(\eta)\right)\\ &+\frac{1}{(T_0-T_w)C_p}\left(\frac{Q^2}{a_0^2 z^2}\frac{1}{\delta^{m+1}}\right)\left(f'(\eta)\right)^2+\frac{\sigma B_0^2}{\mu_0(T_0-T_w)C_p}\frac{Q^2}{z^2\delta^{m+1}}f^2(\eta)\\ &+\frac{D_m K_t}{\nu C_p C_s}\frac{C_0-C_w}{T_0-T_w}\left(\frac{1}{a_0^2}\omega''(\eta)_c+\frac{1}{a_0^2\eta}\omega'(\eta)_c\right) \end{aligned} \tag{2.9}$$

$$\begin{aligned} &-\frac{\mu_0 a_0^{m-1}(m+1)}{\rho\delta^{2(m+1)}}\lambda\omega(\eta)_c=D_m\left(\frac{1}{a_0^2}\frac{\omega''(\eta)_c}{\delta^{m+1}}+\frac{1}{a_0^2\eta}\frac{\omega'(\eta)_c}{\delta^{m+1}}\right)\\ &+\frac{D_m K_t}{T_m a_0^2}\frac{T_0-T_w}{C_0-C_w}\left(\frac{\omega''(\eta)}{\delta^{m+1}}+\frac{1}{\eta}\frac{\omega'(\eta)}{\delta^{m+1}}\right)-\frac{\Gamma\mu_0}{\rho a_0^2}\frac{\omega(\eta)_c}{\delta^{m+1}} \end{aligned} \tag{2.10}$$

We introduce dimensionless parameters which arise from the problem as listed below

$$\begin{aligned} &Re=\frac{Ua}{\nu}, Pr=\frac{C_p\mu}{\kappa}, Ec=\frac{U^2}{C_p\Delta T}, Ha=a_0B_0\sqrt{\frac{\sigma}{\mu}}, Gr=\frac{g\beta^t(T_w-T_0)a_0^3}{\nu^2},\\ &Gc=\frac{g\beta^c(C_w-C_0)a_0^3}{\nu^2}, Sc=\frac{\mu}{\rho D_m}, Sr=\frac{D_m K_t(T-T_w)}{T_m(C-C_w)\nu},\\ &Du=\frac{D_m K_t(C-C_w)}{C_p C_s(T-T_w)\nu}, \Gamma=k_r\frac{\rho a^2}{\mu}, \lambda=\frac{\rho\delta^m}{\mu a^{m-1}}\frac{\mathrm{d}\delta}{\mathrm{d}t}. \end{aligned} \tag{2.11}$$

where *Re* is Reynolds number, *Pr* is Prandtl number, *Ec* is Eckert number, *Ha* is Hartmann number, *Gr* is Thermal Grashof number, *Gc* is Concentration Grashof number, *Sc* is Schmidt number, *Sr* is Soret number, λ is Unsteadiness parameter and *Du* is Dufour parameter.

By substituting Equation (2.11), in Equations (2.8)-(2.10) the following set of ODEs obtained

$$f''(\eta)+\frac{1}{\eta}f'(\eta)+\frac{a_0^{m+1}(m+1)}{\delta^{m+1}}\lambda f(\eta)-Ha^2 f(\eta) -\frac{z}{a_0^2 Re}\left[\omega(\eta)Gr+\omega(\eta)_c\, Gc\right]=0 \tag{2.12}$$

$$\frac{1}{Pr}\omega''(\eta)+\frac{1}{Pr\eta}\omega'(\eta)+\frac{(m+1)a_0^{m+1}}{\delta^{m+1}}\lambda\omega(\eta)+Du\omega''(\eta)_c +Du\frac{1}{\eta}\omega'(\eta)_c+\frac{Ec}{z^2\delta^{m+1}}\left(f'(\eta)\right)^2+\frac{Ha^2Ec}{z^2\delta^{m+1}}f^2(\eta)=0 \tag{2.13}$$

$$\frac{1}{Sc}\frac{\omega''(\eta)_c}{\delta^{m+1}}+\frac{1}{Sc}\frac{\omega'(\eta)_c}{\eta\delta^{m+1}}+\left(\frac{a_0^{m+1}(m+1)}{\delta^{2(m+1)}}\lambda-\Gamma\frac{1}{\delta^{m+1}}\right)\omega(\eta)_c +Sr\frac{\omega''(\eta)}{\delta^{m+1}}+Sr\frac{1}{\eta}\frac{\omega'(\eta)}{\delta^{m+1}}=0 \tag{2.14}$$

The transformed Boundary conditions are as follows.

At the centre line:

$$f(0)=-z\delta^{m+1},\quad \omega(0)=\delta^{m+1},\quad \omega(0)_c=\delta^{m+1}\quad \text{if } \eta=0 \tag{2.15}$$

At the wall:

$$f(0)=-z\delta^{m+1},\quad \omega(0)=\delta^{m+1},\quad \omega(0)_c=\delta^{m+1}\quad \text{if } \eta=0 \tag{2.16}$$

The skin friction, the Nusselt number and Sherwood number are defined by [11]

$$C_f=\frac{\tau_w}{\rho U_0^2},\quad Nu=\frac{a_0 q_h}{k(T_0-T_w)},\quad Sh=\frac{a_0 q_m}{D_m(C_0-C_w)} \tag{2.17}$$

where τ_w is the skin shear stress on the surface, q_h is the heat flux, q_m is the mass flux defined by (2.18) below

$$\tau_w=\mu\left.\frac{\partial u}{\partial r}\right|_{r=0},\quad q_h=-\kappa\left.\frac{\partial T}{\partial r}\right|_{r=0},\quad q_m=-D_m\left.\frac{\partial C}{\partial r}\right|_{r=0} \tag{2.18}$$

By substituting Equation (2.7) in (2.17) following obtained

$$C_f=Re^{-1}f'(\eta),\quad Nu=\frac{-\omega'(\eta)}{\delta^{m+1}},\quad Sh=\frac{-\omega'(\eta)_c}{\delta^{m+1}} \tag{2.19}$$

3 Numerical Solution Procedure

The MATLAB boundary value problem solver function is used to find the numerical solutions for the obtained ODEs. Boundary Value Problem 4th Order Collocation (bvp4c) is a MATLAB solver based on the collocation method that involves selecting a set of discrete points or collocation points, in the interval of interest and requiring that the solution satisfies the differential equation at those points. The solver provides continuous solution with a 4th order accuracy in the interval of integration. Basically the bvp4c function solves and implements a

collocation problem of a two-BVP.

The bvp4c algorithm is the most convenient since it is able to give optimal solutions that are accurate. This algorithm is show below in Figure 2.

Before to the execution of the bvp4c, the higher (second) order nonlinear ODEs are reduced to first order nonlinear ODEs. The following convection are used to reduce the ODEs from the second order to first order ODEs:

$$y_1 = f(\eta), \quad y_2 = f'(\eta), \quad y_3 = \omega(\eta)$$
$$y_4 = \omega'(\eta), \quad y_5 = \omega(\eta)_c, \quad y_6 = \omega'(\eta)_c \tag{3.1}$$

The following system of matrix obtained

$$\begin{bmatrix} y_1' \\ y_2' \\ y_3' \\ y_4' \\ y_5' \\ y_6' \end{bmatrix} = \begin{bmatrix} y_2 \\ Ha^2 y_1 + \dfrac{z}{a_0^2 Re}\left[Gry_3 + Gcy_5\right] - \dfrac{a_0^{m+1}(m+1)\lambda}{\delta^{m+1}} y_1 - \dfrac{1}{\eta} y_2 \\ y_4 \\ -\dfrac{1}{\eta} y_4 - \dfrac{(m+1)a_0^{m+1}\lambda Pr}{\delta^{m+1}} y_3 - DuPry_6' - \dfrac{DuPr}{\eta} y_6 - \dfrac{EcPr}{z^2\delta^{m+1}} y_2^2 - \dfrac{Ha^2 EcPr}{z^2\delta^{m+1}} y_1^2 \quad (\mathbf{S}) \\ y_6 \\ Sc\left[\Gamma - \dfrac{(m+1)a_0^{m+1}}{\delta^{m+1}}\right] y_5 - \dfrac{1}{\eta} y_6 - ScSry_4' - \dfrac{ScSr}{\eta} y_4 \quad (\mathbf{T}) \end{bmatrix} \tag{3.2}$$

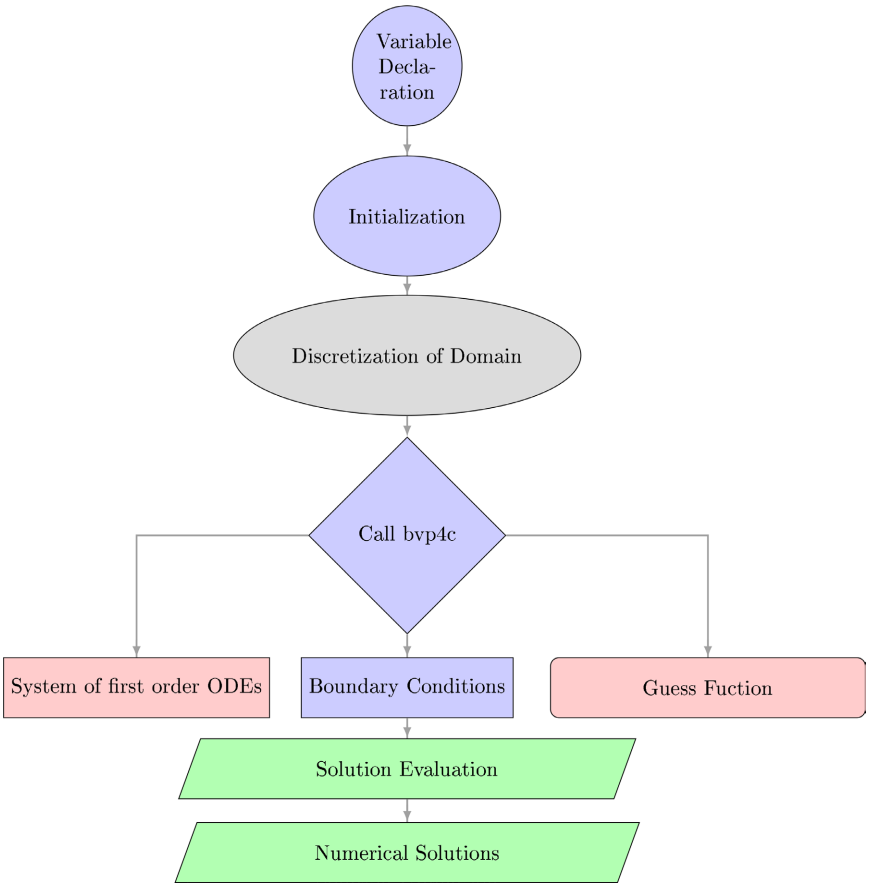

Figure 2. Numerical Scheme for bvp4c.

Where **S** and **T** above become

$$\mathbf{S}=\frac{\left(\frac{DuPrScSr-1}{\eta}\right)y_4-\frac{Pr\lambda(m+1)a_0^{m+1}}{\delta^{m+1}}y_3-DuPrSc\left[\Gamma-\frac{\lambda(m+1)a_0^{m+1}}{\delta^{m+1}}\right]y_5-\frac{EcPr}{z^2\delta^{m+1}}y_2^2-\frac{Ha^2EcPr}{z^2\delta^{m+1}}y_1^2}{1-DuPrScSr} \tag{3.3}$$

$$\mathbf{T}=\frac{\left(\frac{DuPrScSr-1}{\eta}\right)y_6+Sc\left[\Gamma-\frac{\lambda(m+1)a_0^{m+1}}{\delta^{m+1}}\right]y_5+\frac{PrScSr\lambda(m+1)a_0^{m+1}}{\delta^{m+1}}y_3+\frac{PrScSrEc}{z^2\delta^{m+1}}y_2^2+\frac{PrScSrEcHa^2}{z^2\delta^{m+1}}y_1^2}{1-DuPrScSr} \tag{3.4}$$

With the following boundary conditions

$$\text{At centre}: \quad y_1=-z\delta^{m+1}, \quad y_3=\delta^{m+1}, \quad y_5=\delta^{m+1}$$

$$\text{At wall}: \quad y_1=0, \quad y_3=0, \quad y_5=0 \tag{3.5}$$

4. Results and Discussion

The numerical solutions of the model's velocity, temperature, and concentration profiles while varying various dimensionless parameters. The effect of each parameter has been discussed at each stage.

Velocity Profiles

4.1. Effects of Reynolds Number (*Re*) on Velocity

From Figure 3, it observed that velocity of the fluid in the flow region increase with increase in the value of Reynolds number. This is due to the reason that

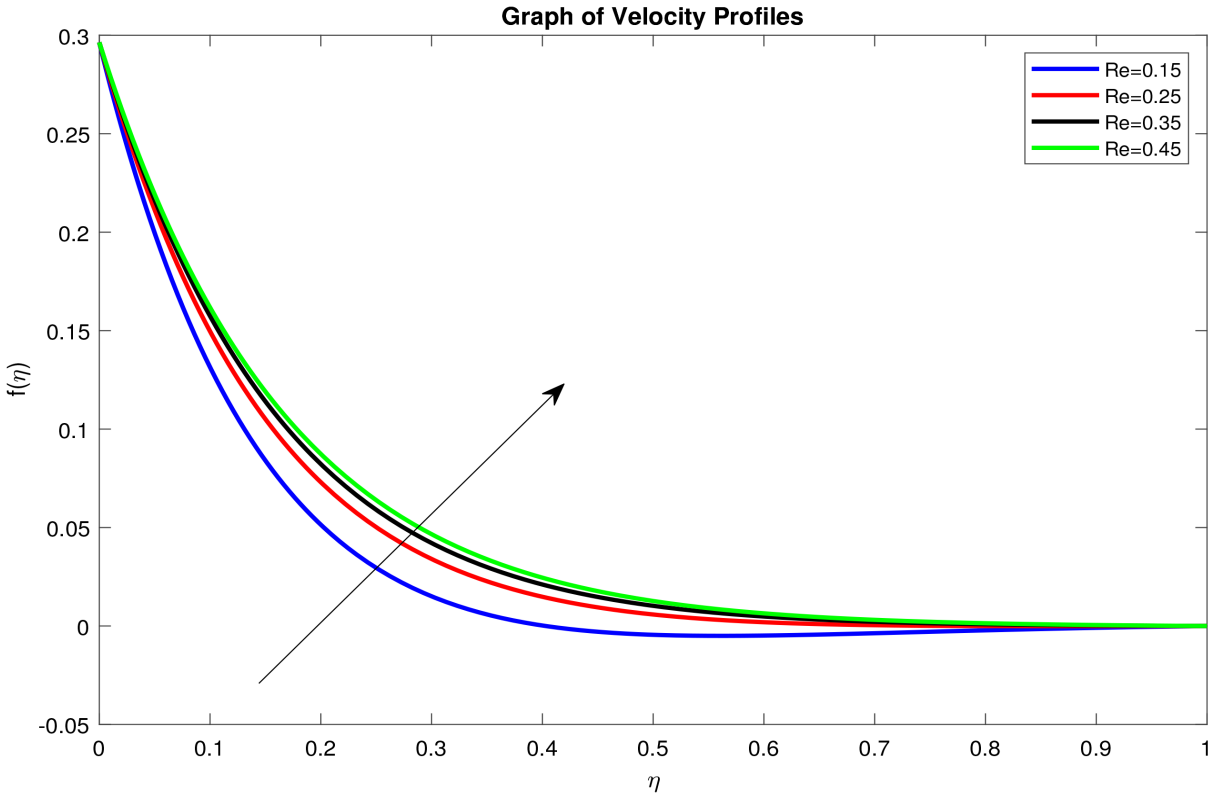

Figure 3. Velocity profiles for different values of *Re*.

increase in Reynolds number leads to decrease of viscosity of the fluid decreases. A decrease in viscosity of the fluid leads to reduce in viscous force in the flow and therefore inertia forces dominates. Since we know that viscous forces tend to oppose the motion of the flowing fluid. Also the velocity boundary layer does not extend more in the free stream region hence increase in fluid velocity. Conversely when viscous forces predominate, Reynolds number reduces leads to decrease in velocity profiles.

4.2. Effects of Hartman Number (*Ha*) on Velocity

In Figure 4 it shows that decrease in Hartman number leads to increase in velocity profiles. An increase in Hartman number leads to decrease velocity of the fluid, this is due to the fact that the presence of uniform magnetic field applied perpendicular to the flow direction of electrically conducting fluid leads to induction of Lorentz force. When Hartman increase causes the increase in the Lorentz force which is against the fluid flow direction causes the fluid's flow to slow down.

4.3. Effects of Unsteadiness Parameter (λ) on Velocity

Considering velocity profile Figure 5 it has been observed that increase in unsteadiness parameter increases velocity profiles. An increase in unsteadiness parameter leads to reduce kinematic viscosity. Hence increase in fluid velocity.

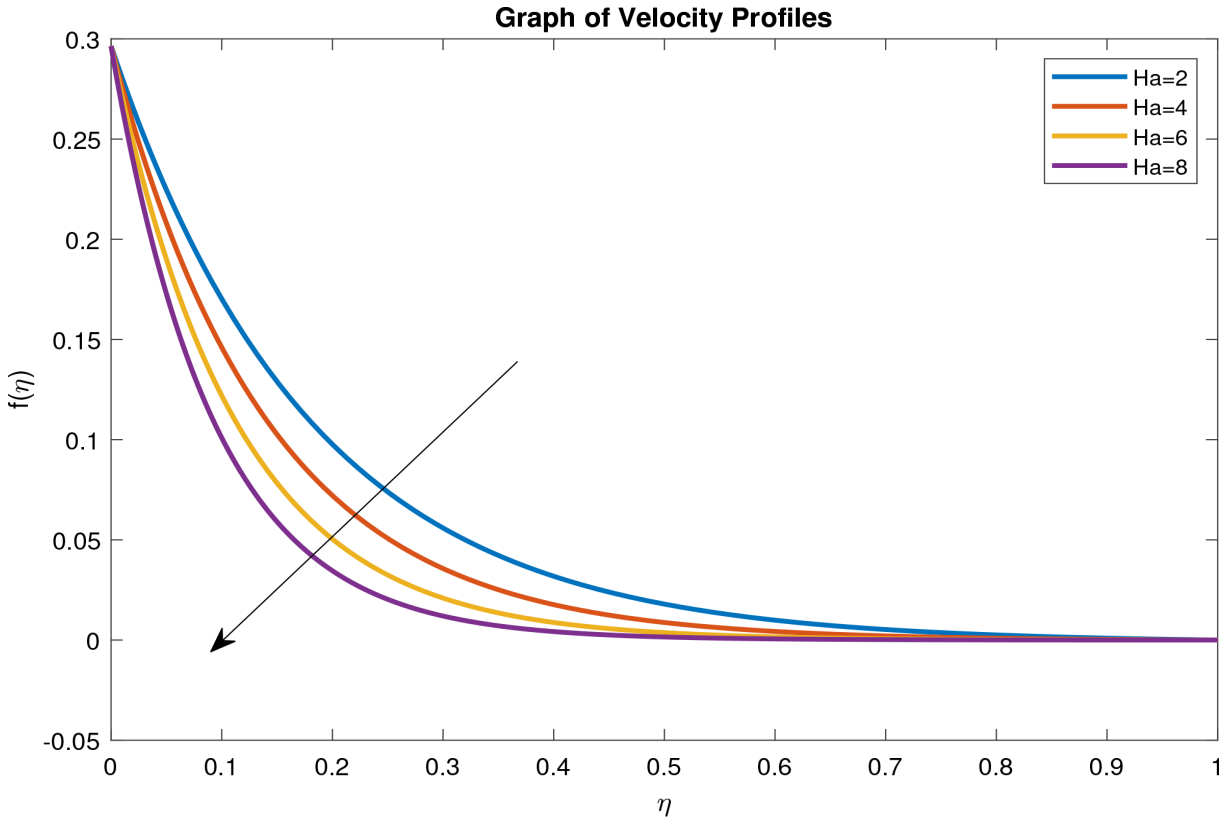

Figure 4. Velocity profiles for different values of *Ha*.

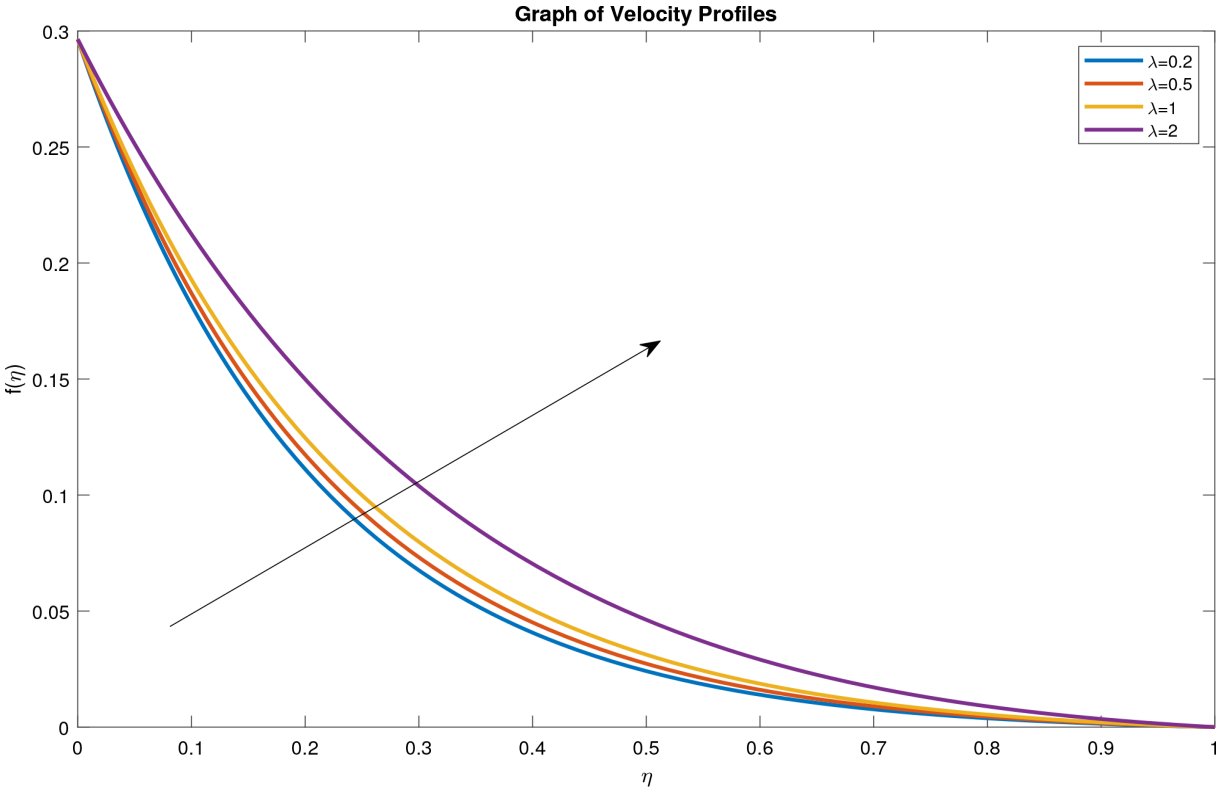

Figure 5. Velocity profiles for different values of λ.

Unsteadiness parameter brings about the issue of unsteady state of the flow and time-dependent scale.

4.4. Effects of Thermal Grashof Number (*Gr*) on Velocity

From Figure 6, it observed that velocity profiles increases as Grashof number for heat transfer increases. From definition of Grashof number for heat transfer is a ratio of the thermal buoyancy force to the viscous force. So when Grashof number increase lead to decrease in viscosity then viscous force hence increase in thermal bouyancy force which lead to an increase in velocity.

4.5. Effects of Concentration Grashof number (*Gc*) on Velocity Profiles

From Figure 7, it has been shown that the velocity of the fluid increases with an increase in the Grashof number for mass transfer (Gc). Since Grashof number for mass transfer is represented by ratio of the species buoyancy force to the viscous force. Increasing Grashof number leads to decrease in the viscosity of the fluid which results to decrease in the viscous force which leads to an increase in the species buoyancy force and hence increase the velocity profiles.

Temperature Profiles

4.6. Effects of Dufour Number (*Du*) on Temperature

In Figure 8, it has been observed that increase in dufour number results to

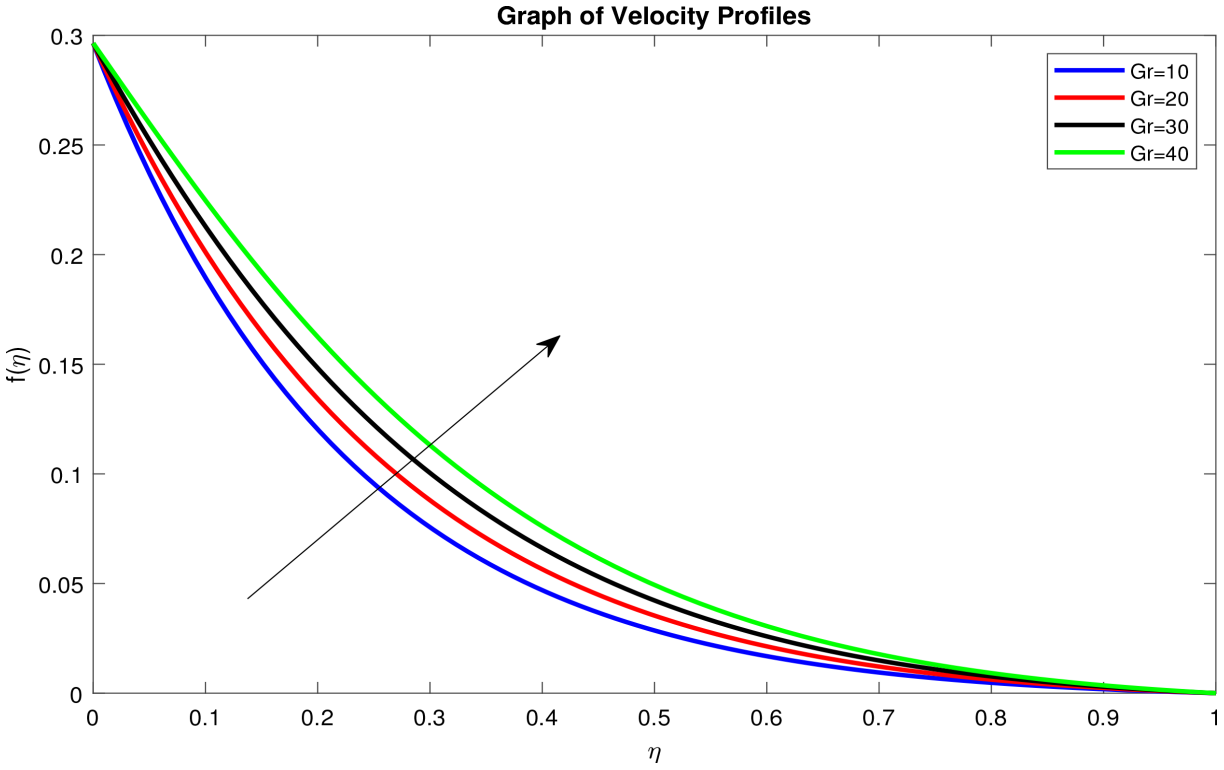

Figure 6. Velocity profiles for different values of *Gr*.

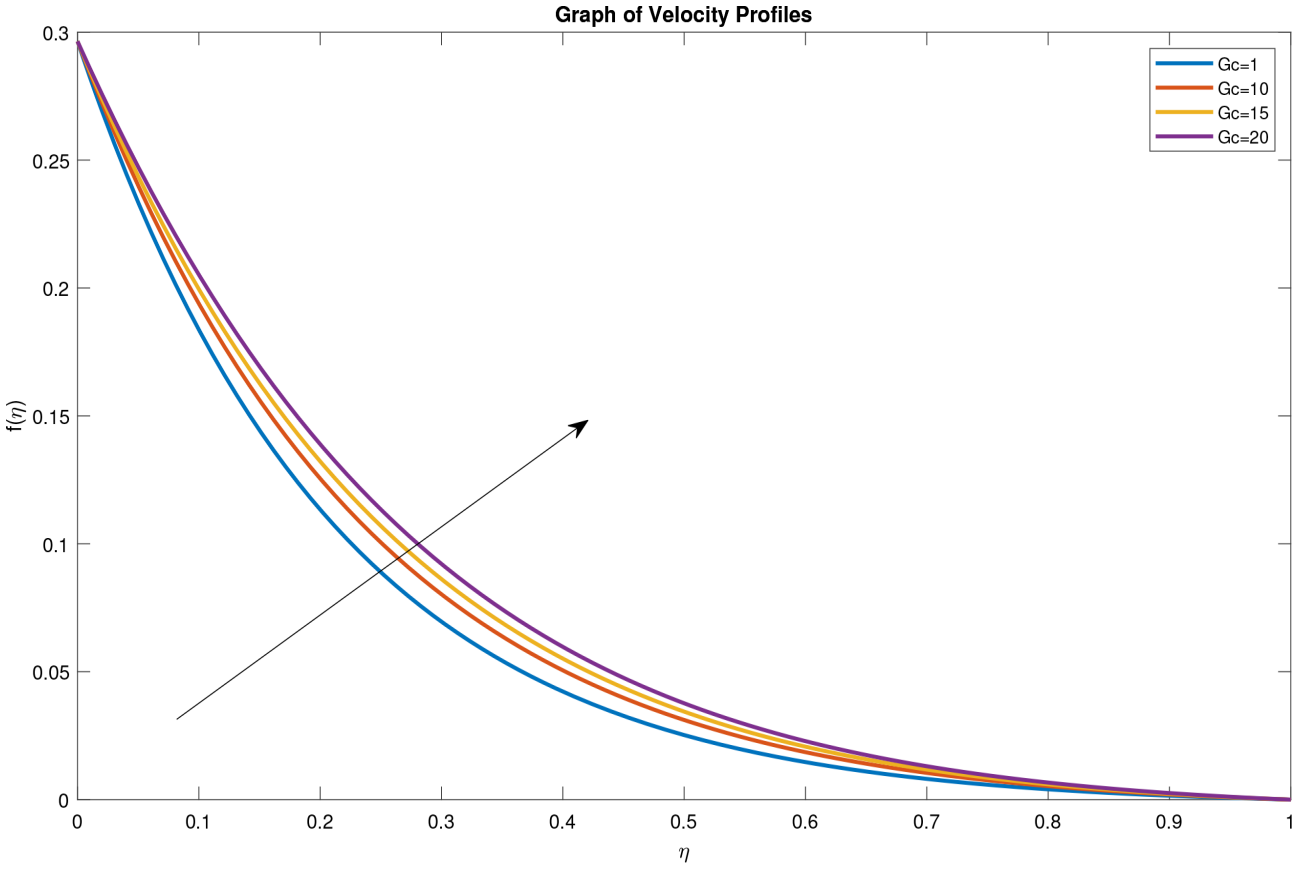

Figure 7. Velocity profiles for different values of *Gc*.

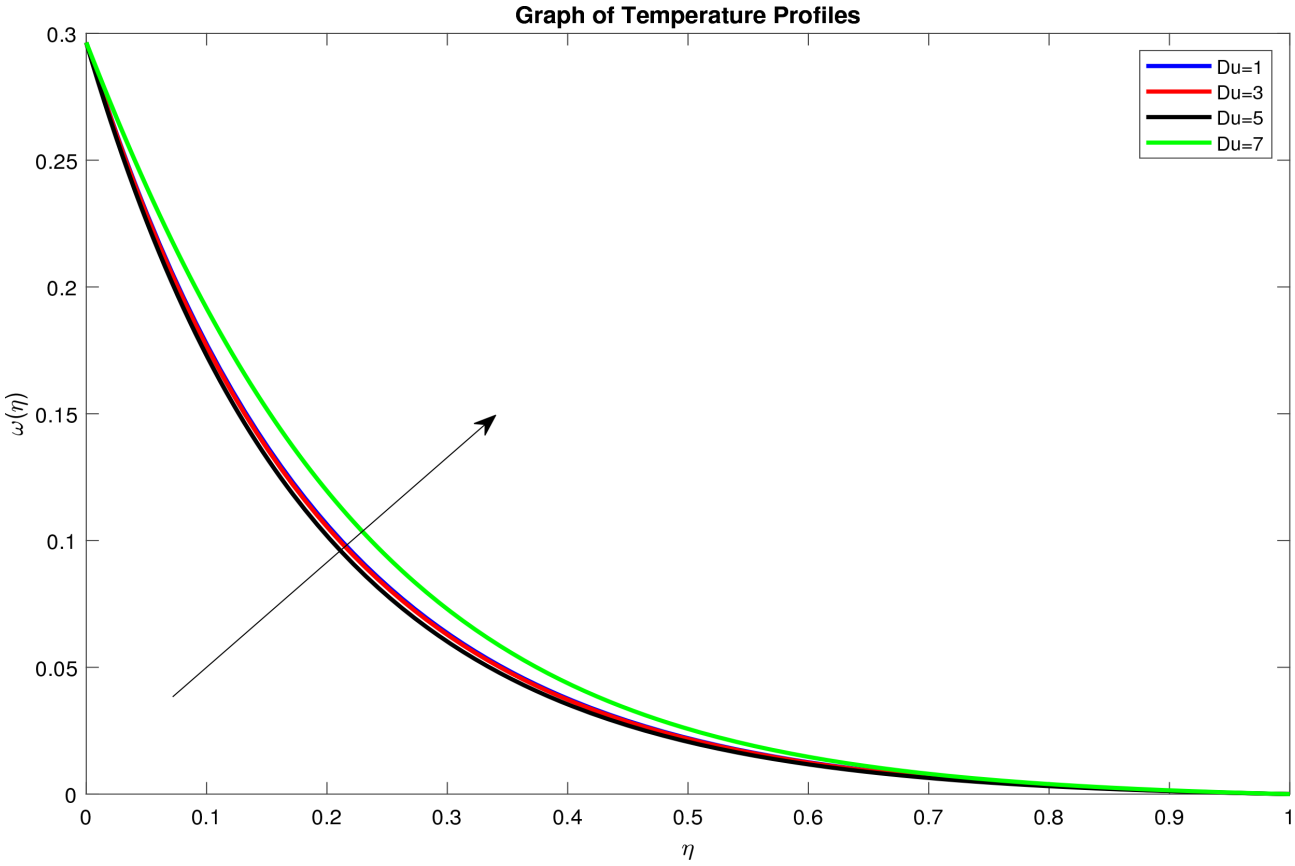

Figure 8. Temperature profiles for different values of *Du*.

increase in temperature profiles. Dufour number is the energy flux (thermal flux) caused by mass concentration gradient, increase in dufour number generate heat flux which lead to increase in thickness of thermal boundary layer this lead slow travel of heat energy, resulting the fluid temperature to rise. This is due to the fact that dufour number is proportional to the temperature differences between wall and fluid.

4.7. Effects of Reynolds Number on Temperature

Figure 9, it found that increase in Reynolds number results into raises in temperature profiles. An increase in Reynolds number leads to the enhanced rates of shearing and consequently the viscous dissipation effects. From literature temperature raises tend to reduce viscous force, thus when viscosity reduce inertia force become predominant since Reynolds parameter is the ratio of the inertial forces to viscous forces. Hence there is direct relation between temperature and Reynolds parameter.

4.8. Effects of Eckert Number (*Ec*) on Temperature

Figure 10 below it shows that an increase in Eckert number leads to raise in temperature profiles. This is because viscous dissipation and joule heating increase as a result of increasing fluid velocity. The velocity is highest at the centre

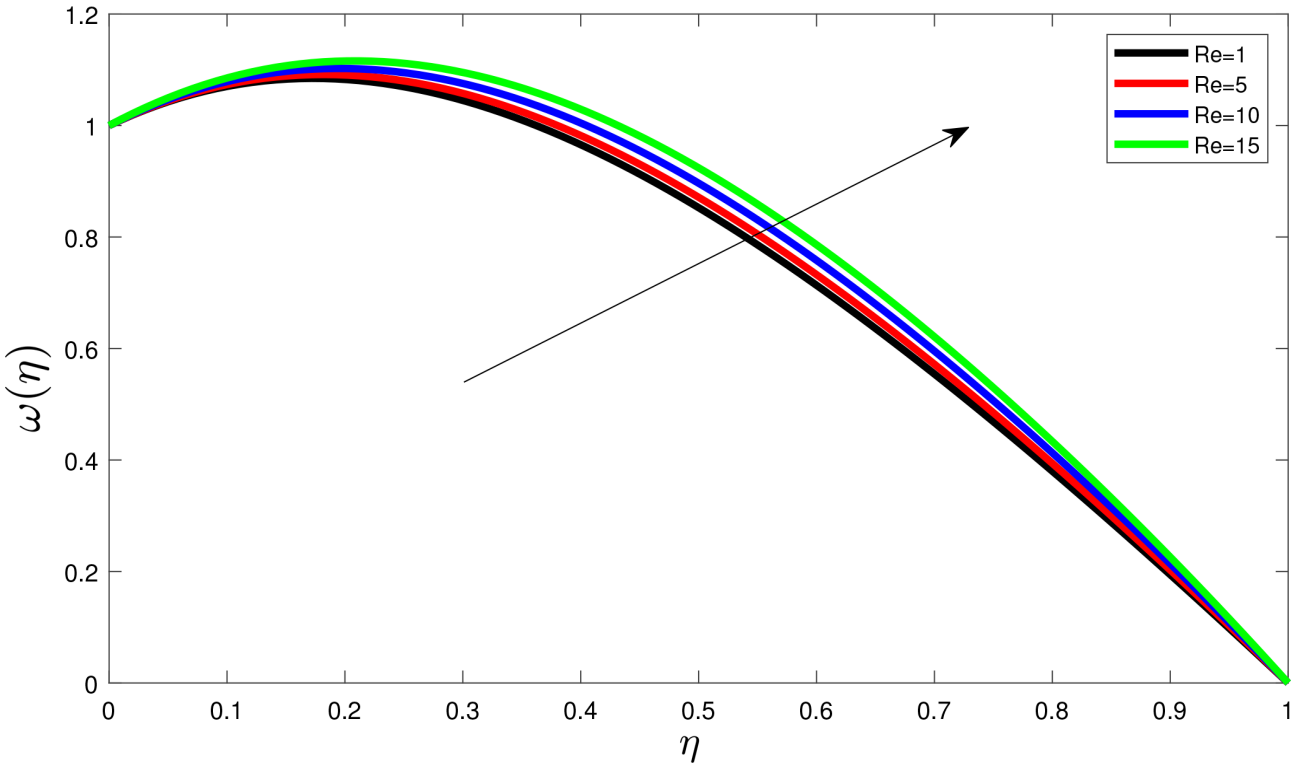

Figure 9. Temperature profiles for different values of *Re*.

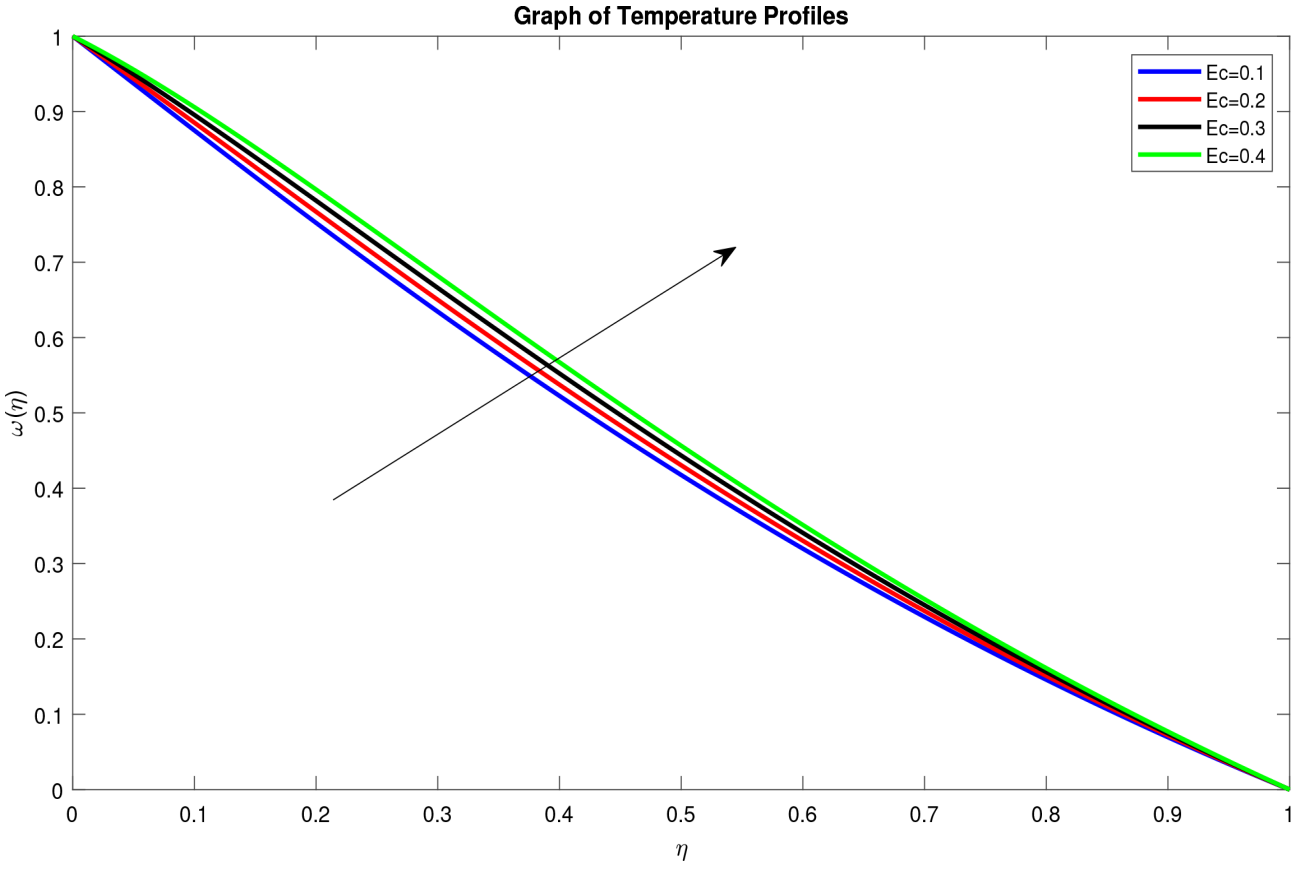

Figure 10. Temperature profiles for different values of *Ec*.

of tube and so viscous dissipation effects. In this case when there is high conversion of kinetic energy into internal energy fluid velocity being high due to fluid particles are in a constant collision and particles vibration becomes high. A rise in the Eckert number translates into increased kinetic energy of the fluid. This increases the motion of the fluids particles which collides and generates energy thereby making the fluids temperature to rise

4.9. Effects of Hartman Number (*Ha*) on Temperature

Figure 11 show that the temperature profiles raises with increase in Hartman number. This increase in Hartman parameter means that magnetic force dominates and viscous forces reduces. The increased magnetic force leads to thermal boundary layer to increase since the thermal boundary layer formed extends into the free stream region which in turn leads to an increased fluid temperature. From literature we know that viscosity and temperature are inversely proportional and when viscosity reduces, this leads to increase of temperature of the fluid flow in the flow region. Also an increase in Hartman number leads to an increase in joule heating from induced electric current. The temperature drops towards the wall of the tube due to the low velocities near the wall which results in the low joule heating.

4.10. Effects of Soret Number (*Sr*) on Temperature

From Figure 12, it is obseved that temperature decreases when soret number increase. This is due to soret number signifies the contribution of the temperature

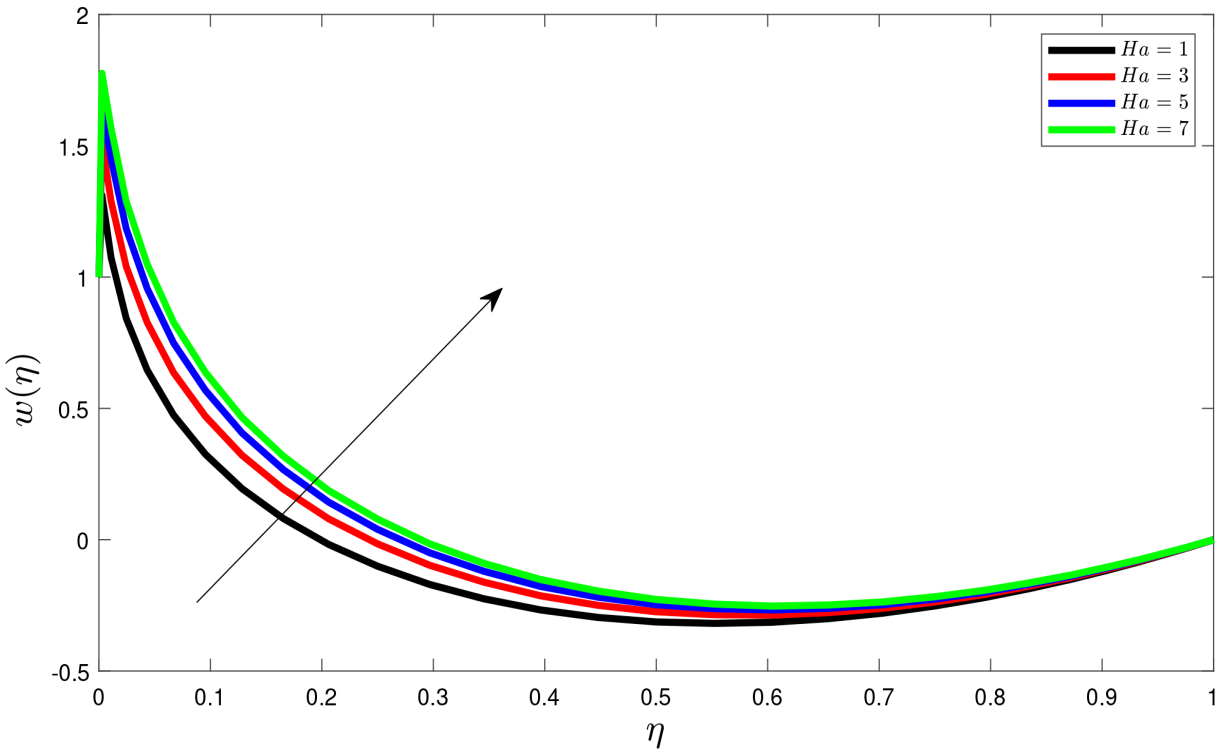

Figure 11. Temperature profiles for different values of *Ha*.

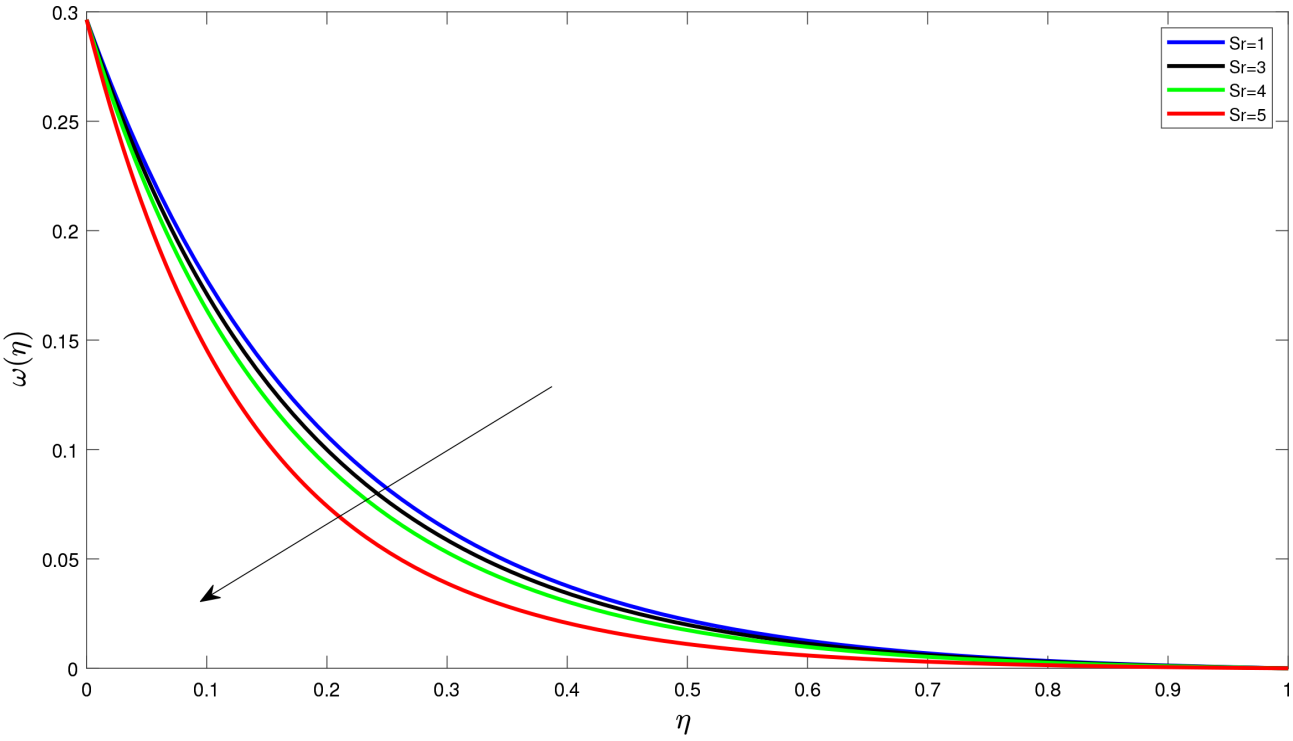

Figure 12. Temperature profiles for different values of *Sr*.

gradient to the mass flux in the fluid flow. Temperature decrease with increase soret number due to it reduce profiles of concentration which leads to increase in mass transfer in the flow.

4.11. Effects of Schmidit (*Sc*) Number on Temperature

From **Figure 13**, it found that an increase in Schmidit number cause a considerable reduction in temperature profiles. From definition Schimdit number is the ratio of kinematic viscosity to the mass diffusitivity. An increase in Schimdit number decrease the mass diffusitivity which leads to increase in viscosity of the fluid and increase in viscocity will results to increase in temperature of the fluid.

Concentration Profiles

4.12. Effects of Dufour Number (*Du*) on Concentration

In **Figure 14** it is noted that when there is decrease in dufour number results into to increase in concentration profiles. This is due to physically as dufour number increases temperature difference between the wall and fluid decreases leads to more heat in fluid. Hence Concentration profiles decrease

4.13. Effects of Chemical Reaction Parameter (Γ) on Concentration

In **Figure 15** it is noted that increase in chemical reaction parameter leads to decrease in concentration profiles. This is due to increase in chemical reaction reduces amount of species in fluid hence the movement of species decrease. When chemical reaction occur species are consumed during reaction process.

Also it is caused by the negative chemical reaction which reduces or decreases the concentration boundary layer thickness and increases the mass transfer.

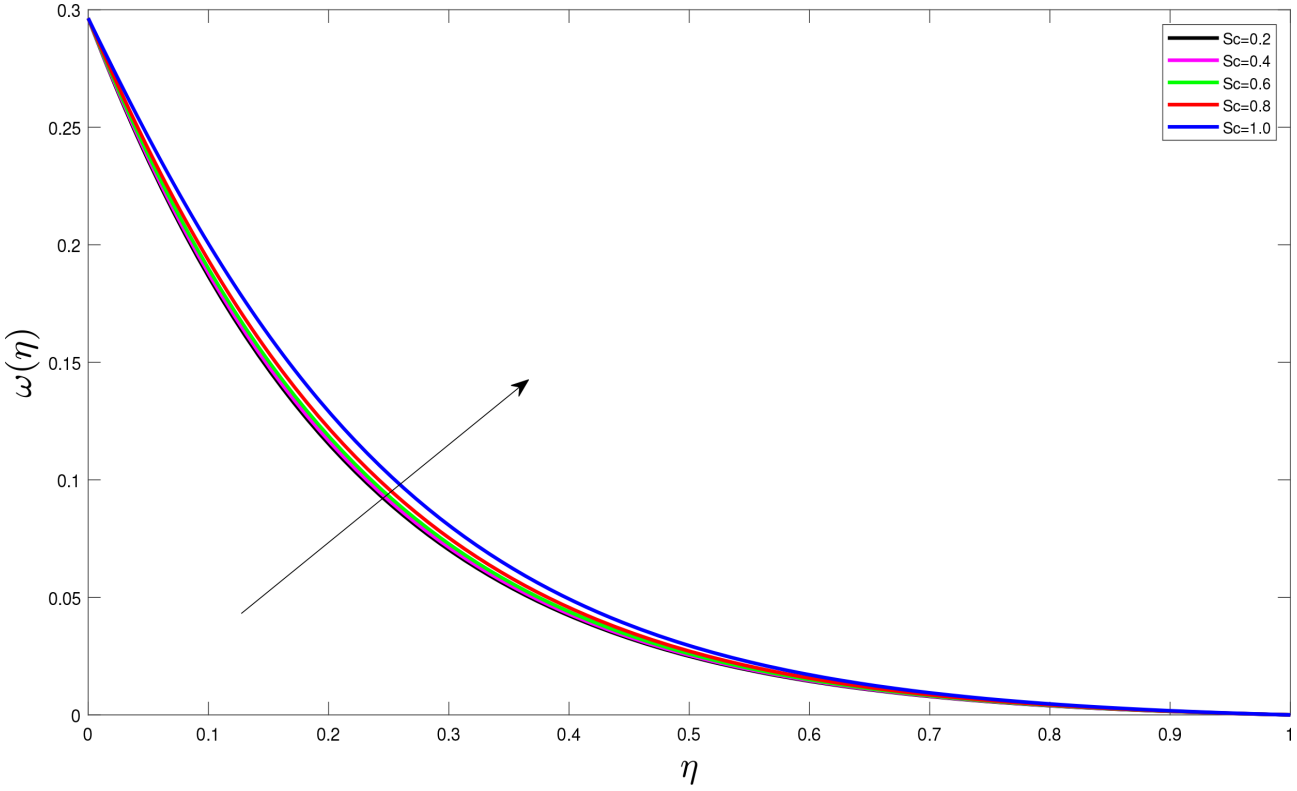

Figure 13. Temperature profiles for different values of *Sc*.

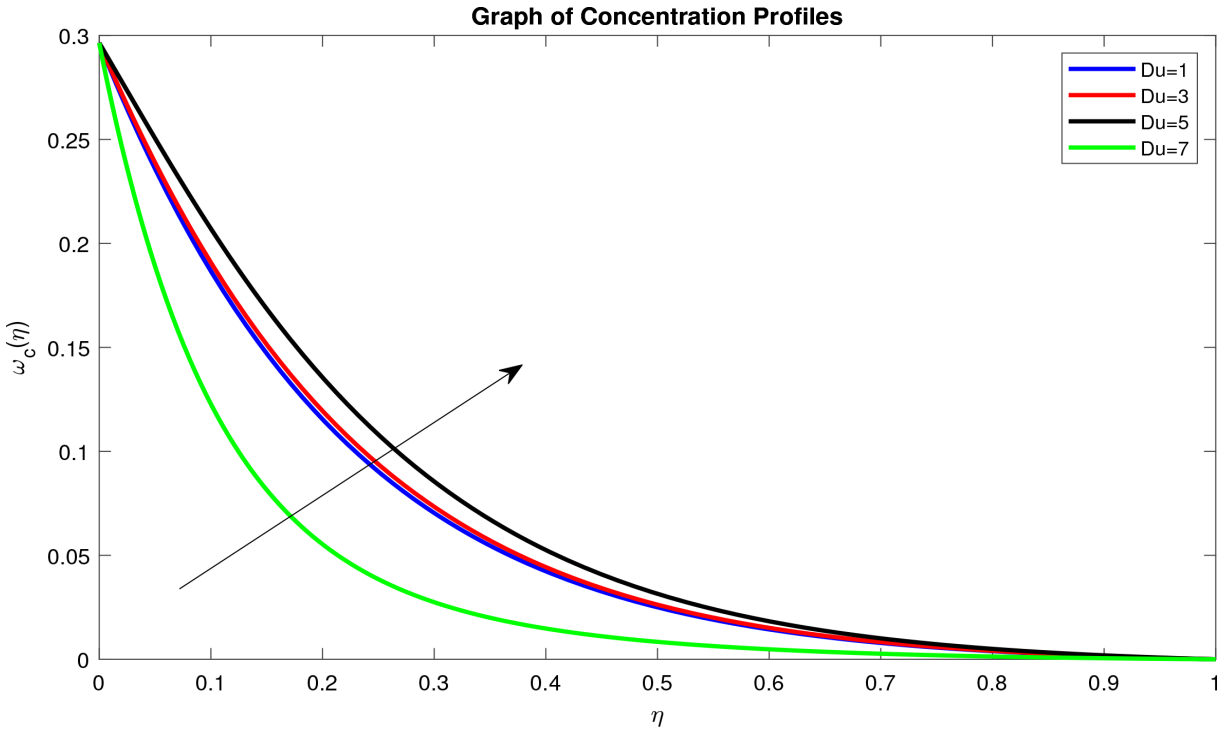

Figure 14. Concentration profiles for different values of *Du*.

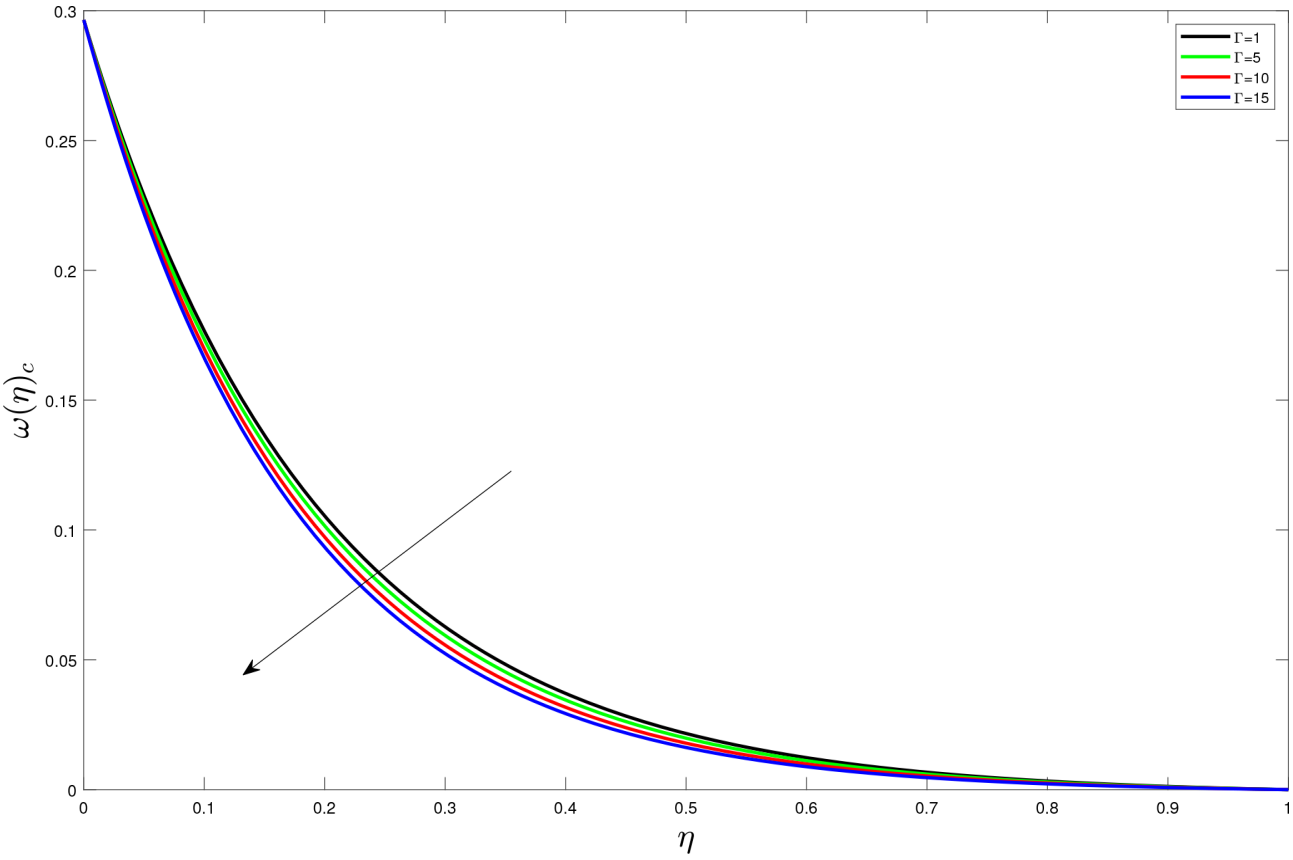

Figure 15. Concentration profiles for different values of Γ.

4.14. Effects of Eckert Number (*Ec*) on Concentration

Figure 16 below, it found that decrease in Eckert number increase concentration profile. An increase in Eckert parameter can lead to enhanced heat transfer, which affects the reaction rates. Higher temperatures resulting from increased heat transfer can accelerate chemical reactions, leading to changes in decreasing concentration profiles. Therefore concentration profiles increase as the results of reducing in Eckert number.

4.15. Effects of Soret Number (*Sr*) on Concentration

In Figure 17, it has been observed that increase in Soret number reduces concentration profiles. Soret number is the mass flux caused by temperature gradient.

4.16. Effects of Schmidit Number (*Sc*) on Concentration

From Figure 18, it is observed that concentration profiles reduced as the Schmidit number increases. This is due to increase in Schmidit number reduces the mass diffusivity as they are in inverse relation which results to decrease in the concentration profiles of the fluid.

4.17. Effects of Concentration Grashof Number (*Gc*) on Concentration

From Figure 19 it observed that increase in Grashof number for mass transfer

leads to decrease concentration profiles. This is due to increase in Grashof number increases in concentration gradient which tend to enhance mass buoyancy effect. The mass buoyanc effect is more at the centre of tube and less

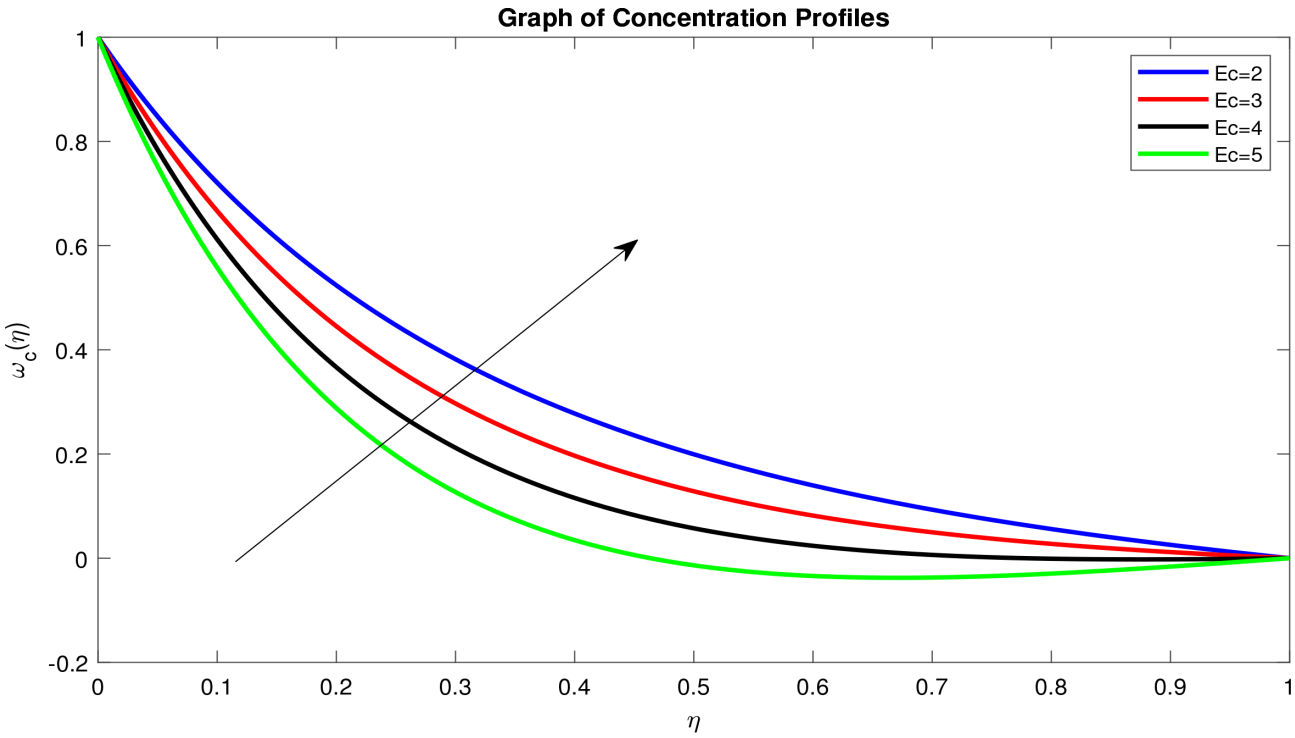

Figure 16. Concentration profiles for different values of *Ec*.

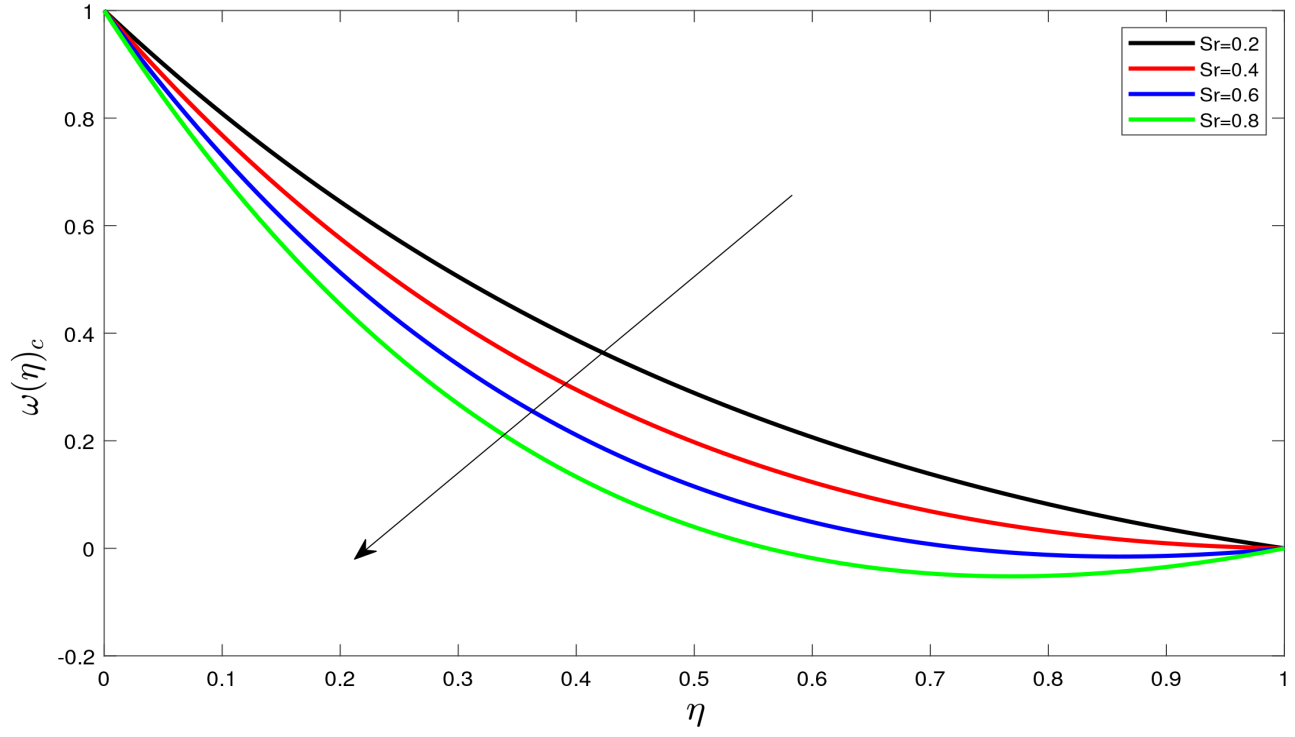

Figure 17. Concentration profiles for different values of *Sr*.

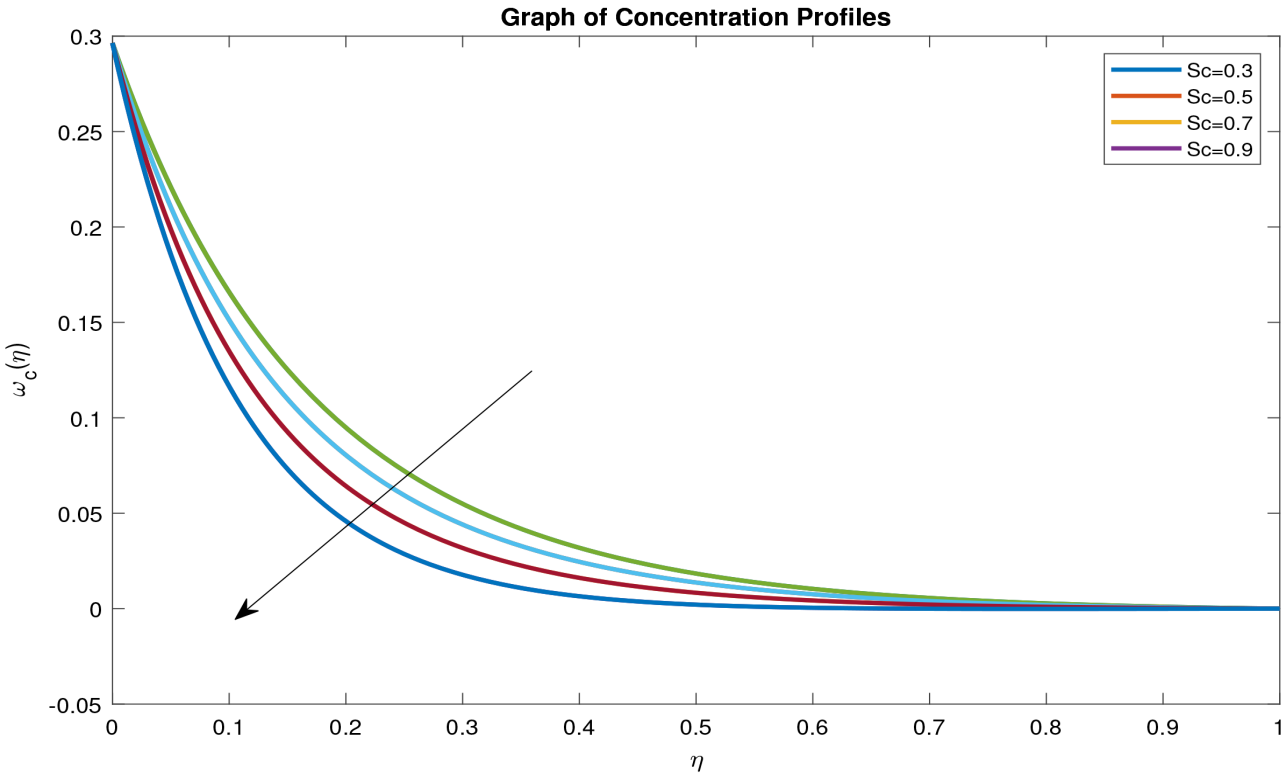

Figure 18. Concentration profiles for different values of *Sc*.

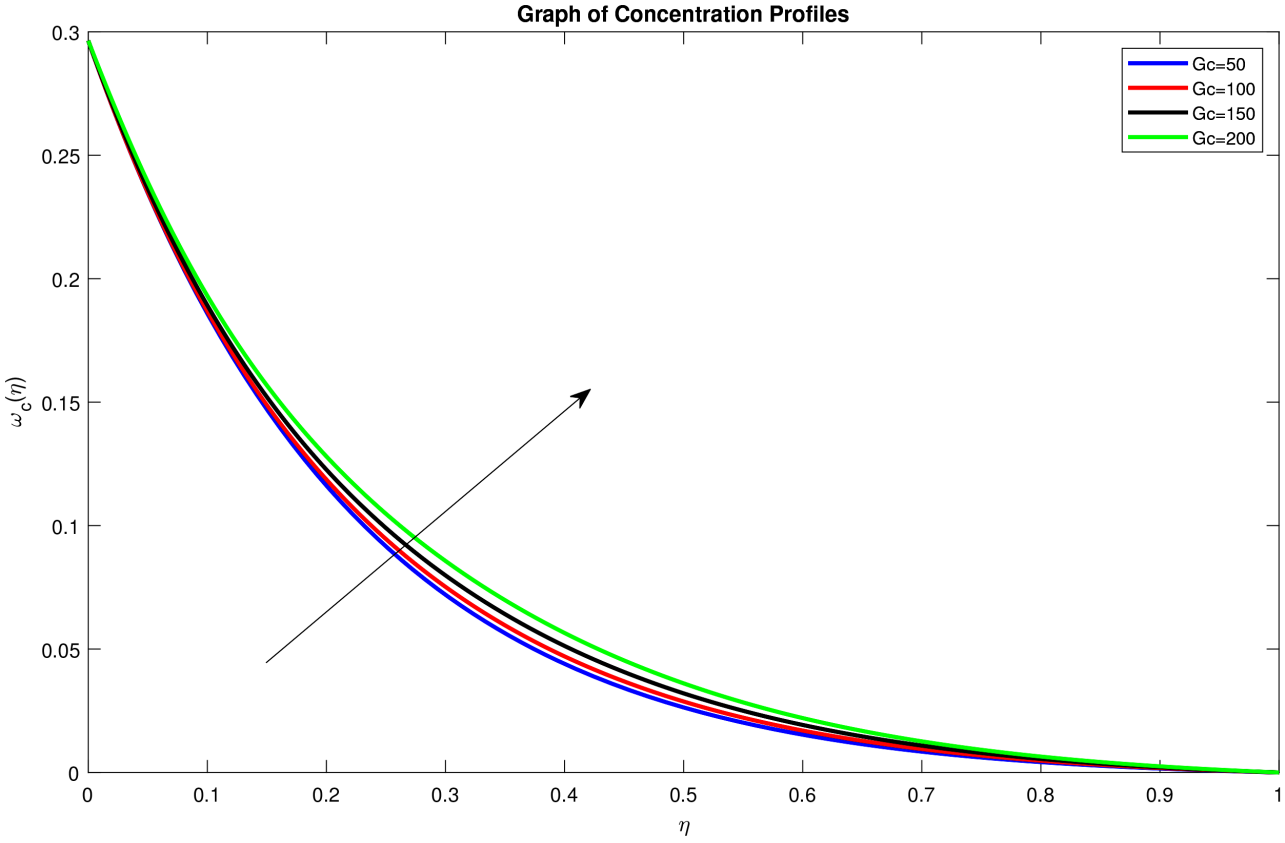

Figure 19. Concentration profiles for different values of *Gc*.

toward the wall then reduces the concentration profiles.

4.18. Effects of Variation of Parameters on Skin Friction

From Table 1, it is noted that increase in the values of Reynolds number, skin friction decreases. This due to the reason that skin friction depend on the viscous forces of the fluid. So the higher the Reynolds number tend to reduce the viscous force hence skin friction reduce. It has been observed that increase in Eckert number and Pradit number there is an increase in skin friction. Also the thermal and concentration Grashof number, Hartman number and unsteadiness parameter increases skin friction as they increase. Furthermore, an increase in the Soret number and Dufour number results in increased skin friction.

Table 1 below shows the results of Skin friction for various values of physical parameters.

4.19. Effects of Variation of Parameters on Heat Transfer Rate

The following are the observable effects of various parameters on Nusselt number as shown in Table 2 below.

Increasing the Prandtl number leads to an increase in the Nusselt number. A low Prandtl number indicates that heat conduction is more influential than convection. When the Prandtl number is high, convection is more effective than pure conduction in transferring energy from an area, so momentum diffusivity is dominant. The Nusselt number increases with an increase in the Eckert number, Reynolds number, Dufour number, unsteadiness parameter and Hartmann number.

There is little or no change in the Nusselt number when the Schmidt number, Soret number, chemical reaction parameter and concentration Grashof number

Table 1. Skin friction coefficient for various values of dimensionless numbers.

Pr	*Ec*	*Sc*	*Sr*	*Re*	Γ	*λ*	*Gr*	*Gc*	*Du*	*Ha*	*Cf*
0.71	0.22	0.2	1	3	0.1	0.1	1	1	1	1	0.5219096
2	0.22	0.2	1	3	0.1	0.1	1	1	1	1	0.5247935
0.71	**5**	0.2	1	3	0.1	0.1	1	1	1	1	0.5267075
0.71	0.22	**1.5**	1	3	0.1	0.1	1	1	1	1	0.5230474
0.71	0.22	0.2	**2**	3	0.1	0.1	1	1	1	1	0.52188582
0.71	0.22	0.2	1	**5**	0.1	0.1	1	1	1	1	0.3101531
0.71	0.22	0.2	1	3	**1.5**	0.1	1	1	1	1	0.5218948
0.71	0.22	0.2	1	3	0.1	**1**	1	1	1	1	0.4629746
0.71	0.22	0.2	1	3	0.1	0.1	**10**	1	1	1	0.5797684
0.71	0.22	0.2	1	3	0.1	0.1	1	**10**	1	1	0.5763336
0.71	0.22	0.2	1	3	0.1	0.1	1	1	**2**	1	0.5762769
0.71	0.22	0.2	1	3	0.1	0.1	1	1	0.1	**1.2**	0.5832763

are altered.

However, the Nusselt number slightly decreases when the thermal Grashof number increased.

4.20. Effects of Variation of Parameters on Mass Transfer Rate

It has been shown in Table 3 that when the Prandtl number, chemical reaction parameter or the dufour parameter is raised, the Sherwood number is reduced. On the other hand, the Sherwood number is enhanced when the Eckert, Schmit,

Table 2. Heat transfer for various values of dimensionless numbers.

Pr	*Ec*	*Sc*	*Sr*	*Re*	Γ	*λ*	*Gr*	*Gc*	*Du*	*Ha*	*Nu*
0.71	0.22	0.2	1	3	0.1	0.1	1	1	1	1	−0.9775911
3	0.22	0.2	1	3	0.1	0.1	1	1	1	1	−1.0027663
0.71	**5**	0.2	1	3	0.1	0.1	1	1	1	1	−1.0164227
0.71	0.22	**1.5**	1	3	0.1	0.1	1	1	1	1	−0.9731386
0.71	0.22	0.2	**2**	3	0.1	0.1	1	1	1	1	−0.9780804
0.71	0.22	0.2	1	**5**	0.1	0.1	1	1	1	1	−0.9795281
0.71	0.22	0.2	1	3	**1.5**	0.1	1	1	1	1	−0.9777634
0.71	0.22	0.2	1	3	0.1	**1**	1	1	1	1	−0.9795529
0.71	0.22	0.2	1	3	0.1	0.1	**10**	1	1	1	−0.9778123
0.71	0.22	0.2	1	3	0.1	0.1	1	**10**	1	1	−0.9779078
0.71	0.22	0.2	1	3	0.1	0.1	1	1	**2**	1	−0.9783239
0.71	0.22	0.2	1	3	0.1	0.1	1	1	0.1	**1.2**	−0.9778536

Table 3. Mass transfer for various values of dimensionless numbers.

Pr	*Ec*	*Sc*	*Sr*	*Re*	Γ	*λ*	*Gr*	*Gc*	*Du*	*Ha*	*Sh*
0.71	0.22	0.2	1	3	0.1	0.1	1	1	1	1	−0.9743499
2	0.22	0.2	1	3	0.1	0.1	1	1	1	1	−0.9723692
0.71	**5**	0.2	1	3	0.1	0.1	1	1	1	1	−0.9809951
0.71	0.22	**1.5**	1	3	0.1	0.1	1	1	1	1	−1.008994
0.71	0.22	0.2	**2**	3	0.1	0.1	1	1	1	1	−0.9736637
0.71	0.22	0.2	1	**5**	0.1	0.1	1	1	1	1	−0.9744119
0.71	0.22	0.2	1	3	**1.5**	0.1	1	1	1	1	−0.9741096
0.71	0.22	0.2	1	3	0.1	**1**	1	1	1	1	−0.9745738
0.71	0.22	0.2	1	3	0.1	0.1	**10**	1	1	1	−0.9743552
0.71	0.22	0.2	1	3	0.1	0.1	1	**10**	1	1	−0.9743596
0.71	0.22	0.2	1	3	0.1	0.1	1	1	**3**	1	−0.9740929
0.71	0.22	0.2	1	3	0.1	0.1	1	1	0.1	**1.2**	−0.9743472

or Soret numbers are raised. However, there is little or no effect of the Reynolds number, unsteadiness parameter, Grashof numbers, or Hartmann number on the Sherwood number.

4.21. Validation

Comparison with previous studies available in the literature has been done and an excellent agreement established. These results agree with [28] when there is absence of dufour effect. The findings were When Eckert number (*Ec*) was increased the temperature and velocity profiles increased. Also when magnetic parameter (*Ha*) increase, velocity profile decrease while temperature raised and when Soret number (*Sr*) increased it reduces concentration profiles.

5. Conclusions

This study has investigated Magneto-hydrodynamic flow of an incompressible fluid in a collapsible elastic tube with mass and heat transfer.

This paper has developed model of the mathematical equations governing the fluid flow in a cylindrical collapsible elastic tube. These equations were non-linear partial differential equations which later were converted to non-linear ordinary differential equations and solved using bvp4c in MATLAB. The results have shown that the equations can be used to predict MHD fluid flow through a collabsible elastic tube for different behaviors. The obtained model is significant for the field as it provide framework for understanding and predicting MHD flow in similar systems. However this model of mathematical equations is based on a certain assumptions and limitations.

Also this study has determined the velocity, concentration, and temperature profiles of the fluid flow through a cylindrical collapsible tube. The effect of varying various flow parameters on the velocity, concentration and temperature distributions have been determined and the results are presented graphically and it leads to conclusion that:

1) The fluid velocity increase with increase in Reynolds number (*Re*), thermal Grashof number (*Gr*), Soret number (*Sr*), while decrease with increase in Hartman number (*Ha*).

2) The temperature of the fluid increases with increase Reynolds number (*Re*), Eckert number (*Ec*), Hartman number (*Ha*), Schmidt number (*Sc*) while decrease with increase in Dufour number (*Du*) and Soret number (*Sr*).

3) The concentration of the fluid decrease with increase in Dufour number (*Du*), chemical reaction parameter (Γ), Eckert number (*Ec*) whereas increase with an increase in Soret number (*Sr*).

4) The rate of heat transfer increase with an increase in Eckert number (*Ec*), Prandtl number (*Pr*), Hartman number (*Ha*), Unsteadiness parameter (λ). There is a little or no change in the Nusselt number (*Nu*) with change in Soret number (*Sr*), Schmidt number (*Sc*), Reynolds number (*Re*), chemical reaction parameter (Γ) and concentration Grashof number (*Gc*).

5) The Mass transfer rate decrease with increase in Prandtl number (Pr), chemical reaction parameter (Γ) while increase with increase Eckert number (Ec), Schmidt number (Sc) and Soret number (Sr). However no effective change in Hartman number Ha, thermal Grashof number (Gr), Reynolds number (Re) and Unsteadiness parameter (λ).

The results obtained from this study can be used in medicine where by the skin-friction coefficient is very important since it enables regulation of blood pressure, preventing of blood clots which may cause a serious health issue i.e stroke. Hence addressing skin friction-related issues is essential in preventing and managing cardiovascular diseases. Also it can be used in thermotherapy, where controlled heat is used to treat injuries or conditions like muscle pain, arthritis.

Future work can be conducted on steady, three-dimensional, MHD fluid flow of mass and heat transfer through collapsible tube with varying magnetic field for turbulent flow.

Conflicts of Interest

The authors declare no conflicts of interest regarding the publication of this paper.

References

[1] Makinde, O. (2005) Collapsible Tube Flow: A Mathematical Model. *Romanian Journal of Physics*, **50**, 493-506.

[2] Luo, X.Y., Cai, Z.X., Li, W.G. and Pedley, T.J. (2008) The Cascade Structure of Linear Instability in Collapsible Channel Flows. *Journal of Fluid Mechanics*, **600**, 45-76. https://doi.org/10.1017/S0022112008000293

[3] Lakshmi Narayana, P.A. and Murthy, P.V.S.N. (2008) Soret and Dufour Effects on Free Convection Heat and Mass Transfer from a Horizontal Flat Plate in a Darcy Porous Medium. *Journal of Heat Transfer*, **130**, Article ID: 104504. https://doi.org/10.1115/1.2789716

[4] Odejide, S.A., Aregbesola, Y.A.S. and Makinde, O.D. (2008) Fluid Flow and Heat Transfer in a Collapsible Tube. *Romanian Journal of Physics*, **53**, 499-506.

[5] Cheng, C.Y. (2009) Soret and Dufour Effects on Natural Convection Heat and Mass Transfer from a Vertical Cone in a Porous Medium. *International Communications in Heat and Mass Transfer*, **36**, 1020-1024. https://doi.org/10.1016/j.icheatmasstransfer.2009.07.003

[6] Rosar, M.E. and Peskin, C.S. (2001) Fluid Flow in Collapsible Elastic Tubes: A Three-Dimensional Numerical Model. *The New York Journal of Mathematics*, **7**, 281-302.

[7] Marchandise, E. and Flaud, P. (2010) Accurate Modelling of Unsteady Flows in Collapsible Tubes. *Computer Methods in Biomechanics and Biomedical Engineering*, **13**, 279-290. https://doi.org/10.1080/10255840903190726

[8] El-Kabeir, S.M.M. (2011) Soret and Dufour Effects on Heat and Mass Transfer Due to a Stretching Cylinder Saturated Porous Medium with Chemically-Reactive Species. *Latin American applied Research*, **41**, 331-337.

[9] Toro, E.F. and Siviglia, A. (2013) Flow in Collapsible Tubes with Discontinuous

Me-Chanical Properties: Mathematical Model and Exact Solutions. *Communications in Computational Physics*, **13**, 361-385. https://doi.org/10.4208/cicp.210611.240212a

[10] Pal, D. and Mondal, H. (2012) Influence of Chemical Reaction and Thermal Radiation on Mixed Convection Heat and Mass Transfer over a Stretching Sheet in Darcian Porous Medium with Soret and Dufour Effects. *Energy Conversion and Management*, **62**, 102-108. https://doi.org/10.1016/j.enconman.2012.03.017

[11] Pal, D. and Chatterjee, S. (2013) Soret and Dufour Effects on MHD Convective Heat and Mass Transfer of a Power-Law Fluid over an Inclined Plate with Variable Thermal Conductivity in a Porous Medium. *Applied Mathematics and Computation*, **219**, 7556-7574. https://doi.org/10.1016/j.amc.2012.10.119

[12] Siviglia, A. and Toffolon, M. (2014) Multiple States for Flow through a collapsible Tube with Discontinuities. *Journal of Fluid Mechanics*, **761**, 105-122. https://doi.org/10.1017/jfm.2014.635

[13] Kanyiri, C.W., Kinyanjui, M. and Giterere, K. (2014) Analysis of Flow Parameters of a Newtonian Fluid through a Cylindrical Collapsible Tube. *SpringerPlus*, **3**, Article No. 566. https://doi.org/10.1186/2193-1801-3-566

[14] Odejide, S.A. (2015) Fluid Flow and Heat Transfer in a Collapsible Tube with Heat Source or Sink. *Journal of the Nigerian Mathematical Society*, **34**, 40-49. https://doi.org/10.1016/j.jnnms.2014.10.003

[15] Mwangi, K.J. (2016) Unsteady Magnetohydrodynamic Fluid Flow in a Collapsible Tube. Ph.D. Thesis, Jomo Kenyatta University of Agriculture and Technology, Juja.

[16] Anand, V. and Christov, I.C. (201) Steady Low Reynolds Number Flow of a Generalized Newtonian Fluid through a Slender Elastic Tube. arXiv: 1810.05155.

[17] Ullah, M.S., Tarammim, A. and Uddin, M.J. (2021) A Study of Two Dimensional Unsteady MHD Free Convection Flow over a Vertical Plate in the Presence of Radiation. *Open Journal of Fluid Dynamics*, **11**, 20-33. https://doi.org/10.4236/ojfd.2021.111002

[18] James, I., Uwem, U. and Inyang, E. (2022) A Study of Two Dimensional Unsteady MHD Free Convection Flow over a Vertical Plate in the Presence of Radiation. *Advances in Chemical Engineering and Science*, **12**, 29-39.

[19] Mehdari, A., Agouzoul, M. and Hasnaoui, M. (2018) Analytical Modelling For Newtonian Fluid Flow through an Elastic Tube. *Journal of Mechanics Engineering and Automation*, **8**, 25-29. https://doi.org/10.17265/2159-5275/2018.01.004

[20] Maurice, P., Giterere, K. and Kiongora, R. (2019) Unsteady Flow of a Newtonian Fluid through a Cylindrical Collapsible Tube. *International Journal of Applied Mathematics and Mechanics*, **7**, 1-8.

[21] Chepkonga, D., Kiogora, R. and Giterere, K. (2019) Fluid Flow and Heat Transfer through a Vertical Cylindrical Collapsible Tube in the Presence of Magnetic Field and an Obstacle. *International Journal of Advances in Applied Mathematics and Mechanics*, **71**, 62-71.

[22] Alsemiry, R.D., Mandal, P.K., Sayed, H.M., Amin, N., *et al.* (2020) Numerical Solution of Blood Flow and Mass Transport in an Elastic Tube with Multiple Stenoses. *BioMed Research International*, **2020**, Article ID: 7609562. https://doi.org/10.1155/2020/7609562

[23] Idowu, A.S. and Falodun, B.O. (2020) Effects of Thermophoresis, Soret-Dufour on Heat and Mass Transfer Flow of Magnetohydrodynamics Non-Newtonian Nanofluid over an Inclined Plate. *Arab Journal of Basic and Applied Sciences*, **27**, 149-165. https://doi.org/10.1080/25765299.2020.1746017

[24] Priyadharsini, S. (2020) Unsteady Flow of Collapsible Tube under Transverse Magneto Hydrodynamic Fluid. *International Journal of Advanced Science and Technology*, **29**, 1995-2001.

[25] Ou, X.Y., Wang, R.J., Guo, T.W., Shao, C. and Zhu, Z.F. (2022) Numerical Investigation on the Heat and Mass Transfer in Microchannel with Discrete Heat Sources Considering the Soret and Dufour Effects. *Micromachines*, **13**, Article 1848. https://doi.org/10.3390/mi13111848

[26] Moghimi, S.M., *et al.* (2023) Heat Transfer of MHD Flow over a Wedge with Surface of Mutable Temperature. *Authorea*. https://doi.org/10.22541/au.167425252.22171125/v1

[27] Hussain, F., Nazeer, M., Mengal, A., Hussain, A. and Ali Raza Shah, S. (2023) Numerical Simulation of MHD Two-Dimensional Flow Incorporated with Joule Heating and Nonlinear Thermal Radiation. *ZAMM-Journal of Applied Mathematics and Mechanics/Zeitschrift für Angewandte Mathematik und Mechanik*, **103**, e202100246. https://doi.org/10.1002/zamm.202100246

[28] Mwamba, N., Okelo Abonyo, J., Awuor, K.O., *et al.* (2023) Effects of Thermal Radiation and Chemical Reaction on Hydromagnetic Fluid Flow in a Cylindrical Collapsible Tube with an Obstacle. *International Journal of Mathematics and Mathematical Sciences*, **2023**, Article ID: 9991376. https://doi.org/10.1155/2023/9991376

[29] Ojiambo, V., Kinyanjui, M. and Kimathi, M. (2018) A Study of Two-Phase Jeffery Hamel Flow in a Geothermal Pipe. *International Journal of Advances in Applied Mathematics and Mechanics*, **6**, 21-32.

[30] Wawira, N.C., Kinyanjui, M., Giterere, K., *et al.* (2022) Hydromagnetic Non-Newtonian Fluid Flow in a Convergent Conduit. *Journal of Applied Mathematics*, **2022**, Article ID: 8131528. https://doi.org/10.1155/2022/8131528

Nomenclature

Symbol	Meaning
u_z	Vertical velocity, meters (ms^{-1})
u_θ	Angular velocity, rad (rad s^{-1})
u_r	Radial velocity, meters (ms^{-1})
u	Speed of the fluid, (ms^{-1}).
r	Radius of the tube, meters (m)
a_0	Characteristic radius, meters (m)
z	Axial coordinate, meters (m)
t	Time, seconds (s)
B_0	Constant magnetic field, Tesla (T)
K_t	Thermal diffusion ratio
T	Temperature, kelvin (K)
T_0	Temperature at the center, kelvin (K)
T_w	Temperature at the wall, kelvin (K)
T_m	Mean temperature, kelvin (K)
C	Concentration, mole per cubic meter mol/m^3
C_0	Concentration at the center, mole per cubic meter mol/m^3
C_w	Concentration at the wall, mole per cubic meter mol/m^3
C_s	Concentration Susceptibility
C_p	Specific heat capacity, ($J{\cdot}kg^{-1}{\cdot}K^{-1}$)
D_m	Concentration diffusion parameter, ($m^2{\cdot}s^{-1}$)
k_r	Chemical reaction coefficient, ($M{\cdot}s^{-1}$)
Q	Discharge, ($m^3{\cdot}s^{-1}$)
$f(\eta)$	Dimensionless velocity
P	Pressure, ($N{\cdot}m^{-2}$)
m	Arbitrary constant
I	Electric current, Ampere (A)
J	Electric current density, ($A{\cdot}m^{-2}$)
$\boldsymbol{B}$	Magnetic vector
g	Gravitational constant, ($N{\cdot}m^2{\cdot}kg^{-2}$)
q_h	Heat flux, ($W{\cdot}m^{-2}$)
q_m	Mass flux, ($kg{\cdot}m^{-2}{\cdot}s^{-1}$)
Re	Reynolds number
Pr	Prandtl number
Ec	Eckert number
Ha	Hartmann number

Gr	Thermal Grashof number
Gc	Concentration Grashof number
Sc	Schmidt number
Sr	Soret number
Du	Dufour parameter
C_f	Skin friction coefficient
Nu	Nusselt number
Sh	Sherwood number
α	Thermal diffusion rate
β^c	Volumetric concentration expansion, ($kg{\cdot}m^{-3}$)
β^t	Volumetric thermal expansion, $kelvin{\cdot}K^{-1}$
Γ	Chemical reaction parameter $M{\cdot}s^{-1}$
δ	Time-dependent length scale, M
η	Dimensionless radius
λ	Unsteadiness parameter
μ	Fluid viscosity, $kg{\cdot}m^{-1}{\cdot}s^{-1}$
ρ	Fluid density, $kg{\cdot}m^{-3}$
ϕ	Viscous dissipation, s^{-2}
κ	Thermal conductivity, $W{\cdot}m^{-1}{\cdot}K^{-1}$
τ	Shear stress, $N{\cdot}m^{-2}$
σ	Electrical conductivity, $\Omega^{-1}{\cdot}m^{-1}$
τ_w	Skin shear stress, $N{\cdot}m^{-2}$
θ	Azimuthal angle, rad
$\omega(\eta)$	Dimensionless temperature
$\omega(\eta)_c$	Dimensionless concentration